The Abdus Salam International Centre for Theoretical Physics

United Nations Educational, Scientific and Cultural Organization

IAEA International Atomic Energy Agency

2269-6

Workshop on New Materials for Renewable Energy

17 - 21 October 2011

Computational modeling of materials and processes in hybrid/organic photovoltaics

Filippo DE ANGELIS

Istituto CNR di Scienze e Tecnologie Moleculari ISTM
c/o Dipt. di Chimica, Univ. di Perugia
I-06123 Perugia
Italy

Computational Modeling of Materials and Processes in Hybrid/Organic Photovoltaics

Filippo De Angelis

Istituto CNR di Scienze e Tecnologie Molecolari (ISTM), c/o
Dipartimento di Chimica, Università di Perugia, I-06123 Perugia, Italy

Part I
Photovoltaics

CONVENTIONAL PHOTOVOLTAICS: SILICON

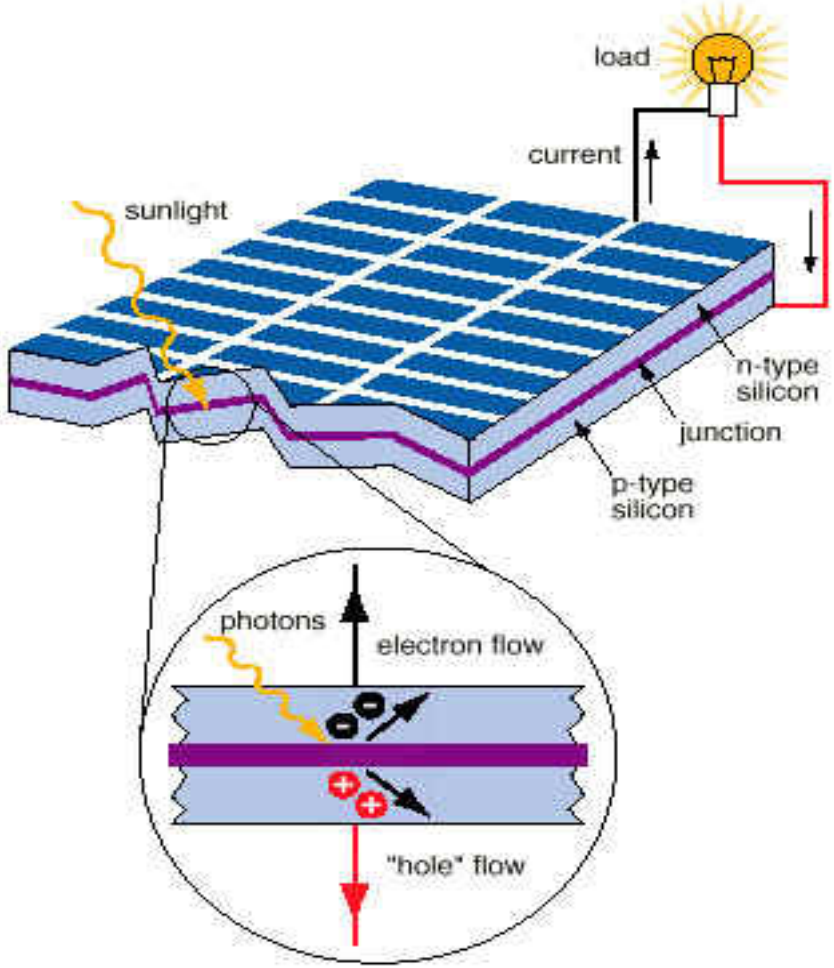

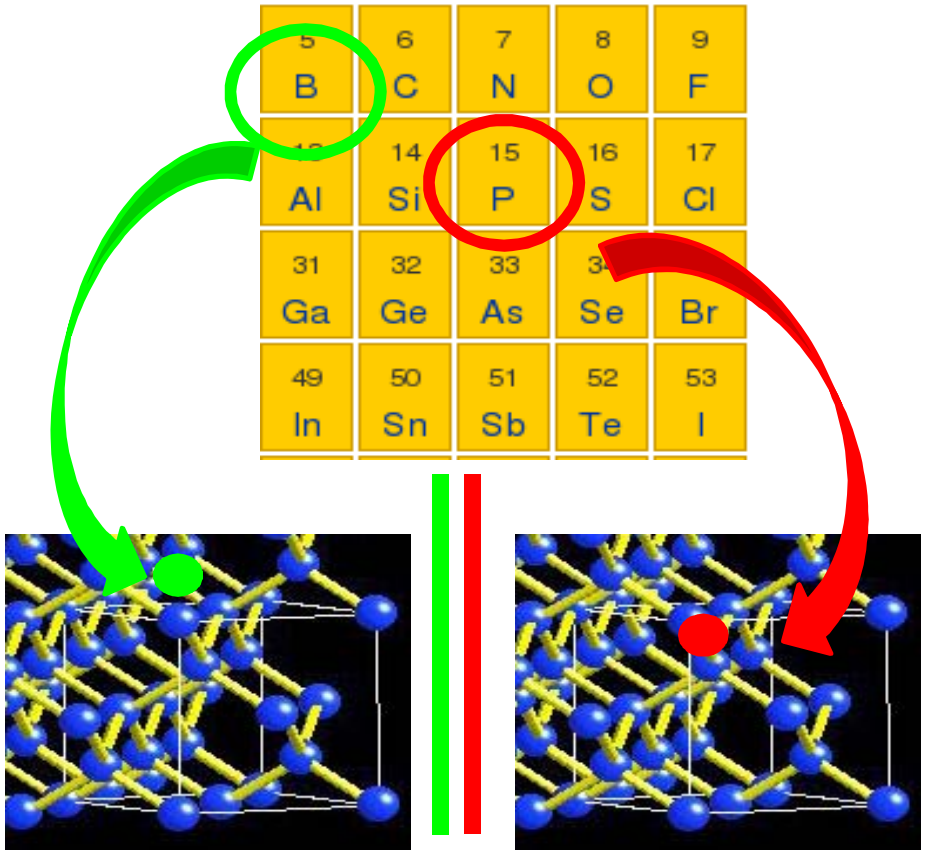

P JUNCTION N

CONVENTIONAL PHOTOVOLTAICS: SILICON
HIGH EFFICIENCY / HIGH PRICE

WHY SILICON ?

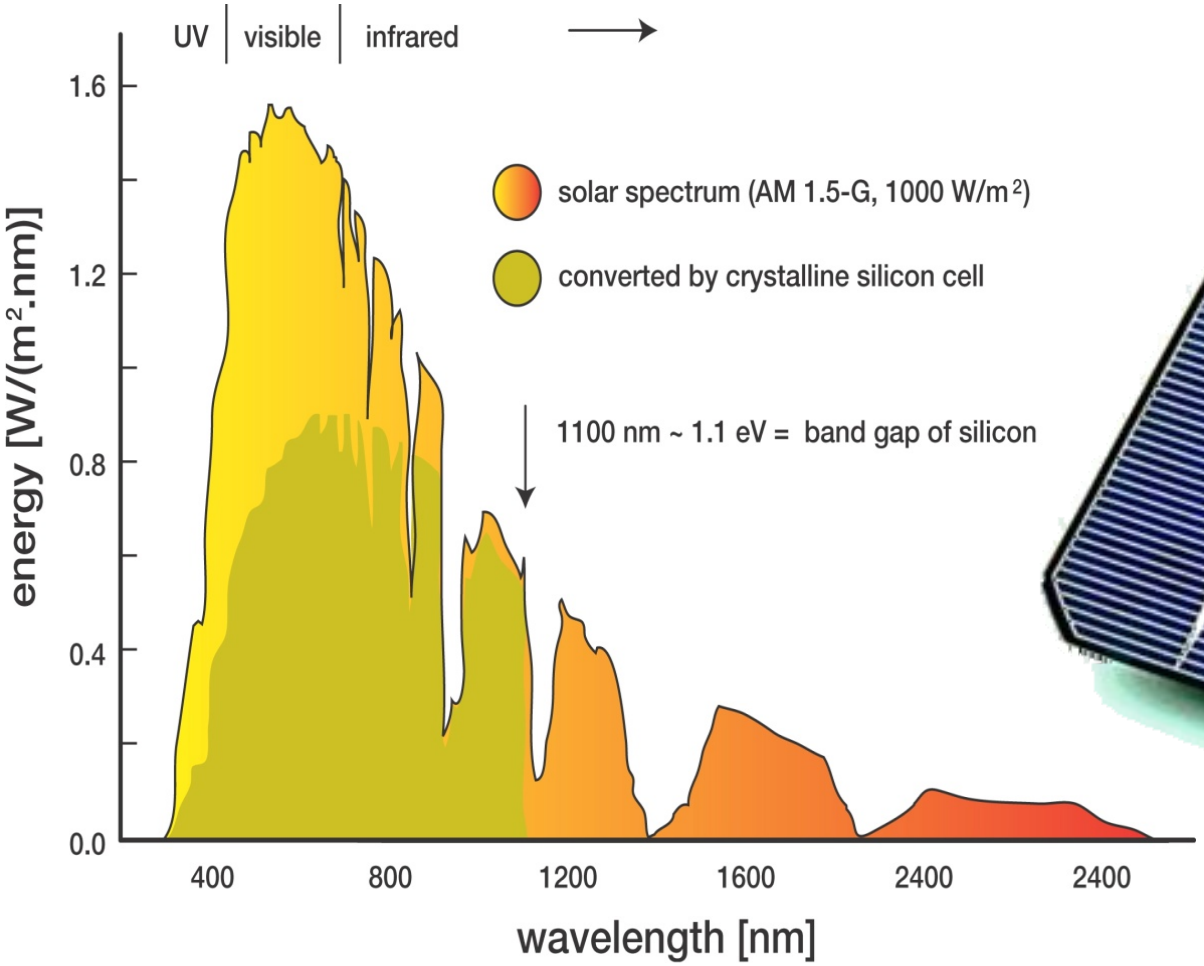

BECAUSE IT' S BLACK!

CAN I USE A DIFFERENT SEMICONDUCTOR?

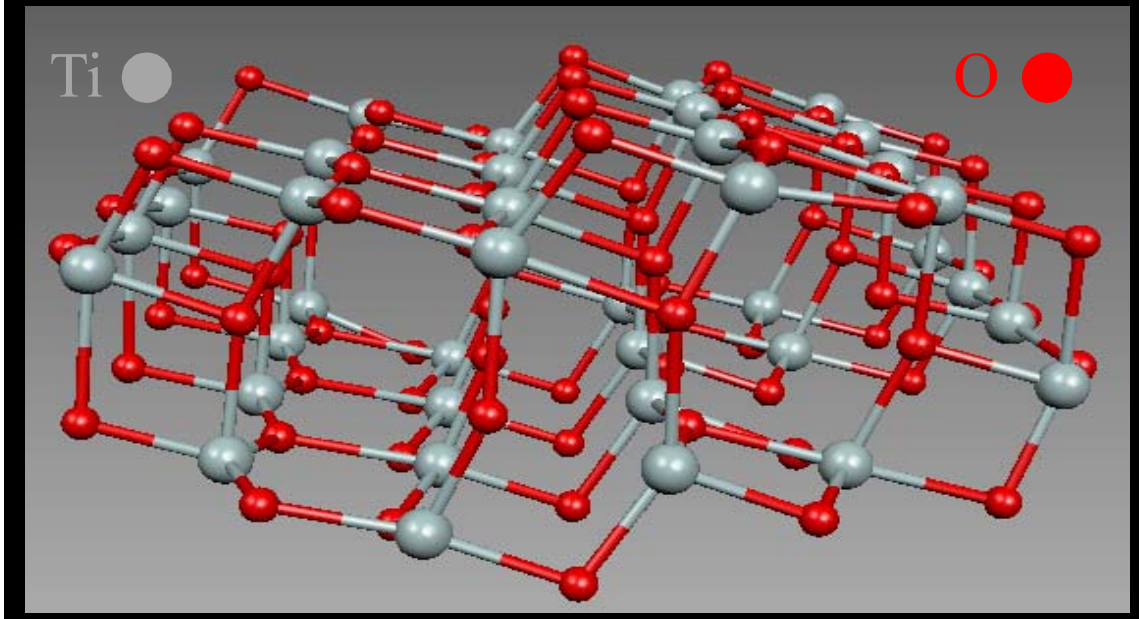

NANOCRYSTALLINE TiO_2

TITANIUM DIOXIDE IS A HIGHLY STABLE SEMICONDUCTOR WITH EXCELLENT ELECTRON MOBILITY

…… BUT

IT'S WHITE!

The problem is to gather solar light at an effective cost!

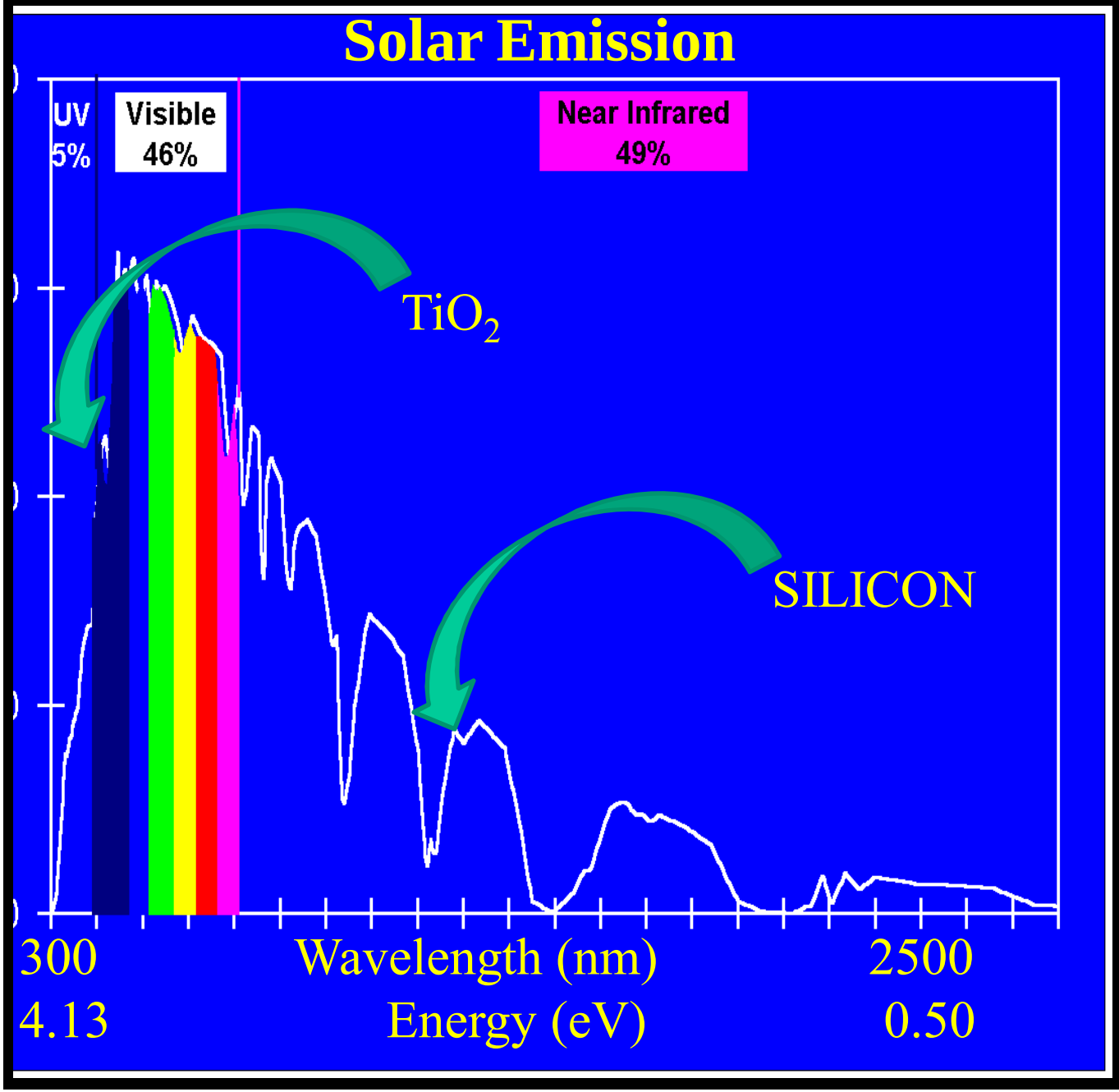

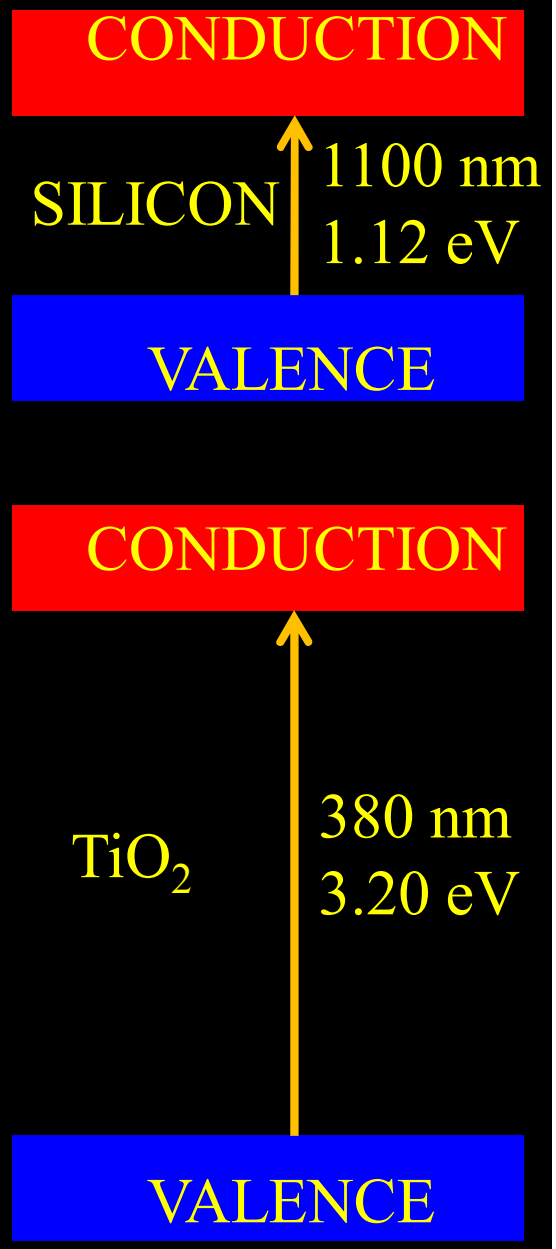

DYE SENSITIZED SOLAR CELLS

NATURAL DYES

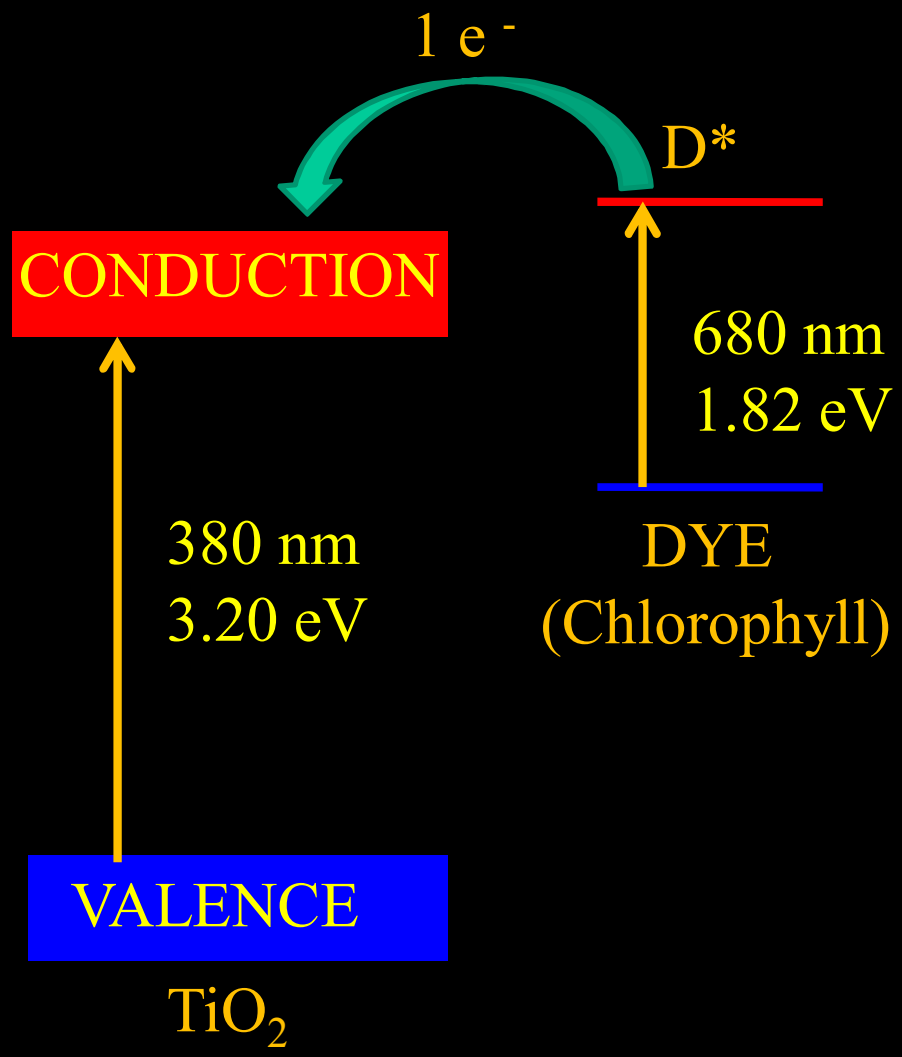

DSC: Principles of operation

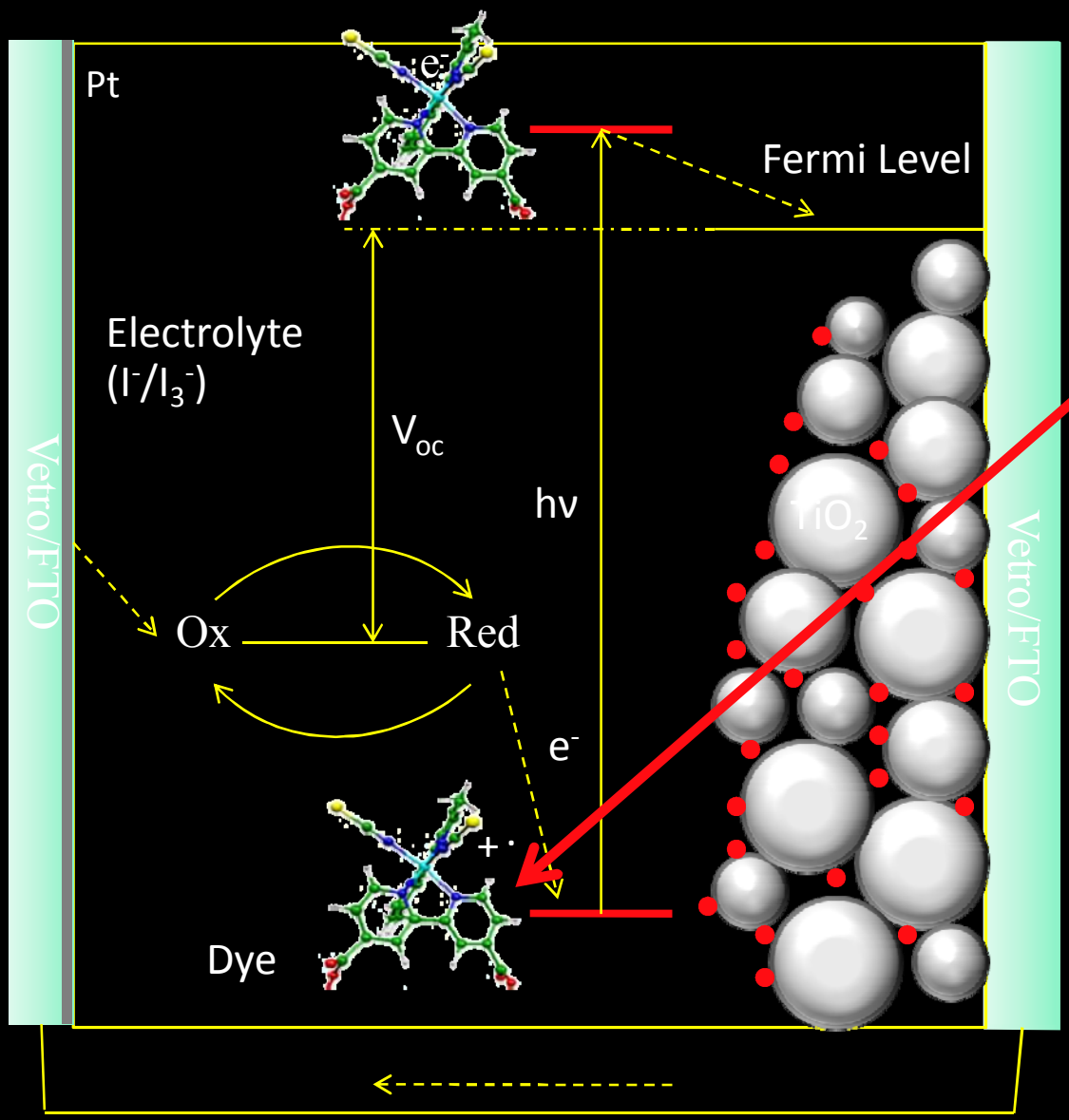

In DSCs TiO_2 nanoparticles are sensitized with a light-harvesting sensitizer and are typically surrounded by a liquid electrolyte.

The dye-sensitizer captures photons and an electron/hole pair is generated.

The electron is injected into conduction band of TiO_2 and then flows into the external circuit.

The oxided dye is regenerated by the redox couple in the electrolyte.

Photocurrent: rate of electron injection (I= dq/dt)

Photovoltage: Position of the conduction band.

M. Grätzel, *Nature*, 2001, **414**, 338

Dye-Sensitized Solar Cells: Flexible, colorful, transparent PVs

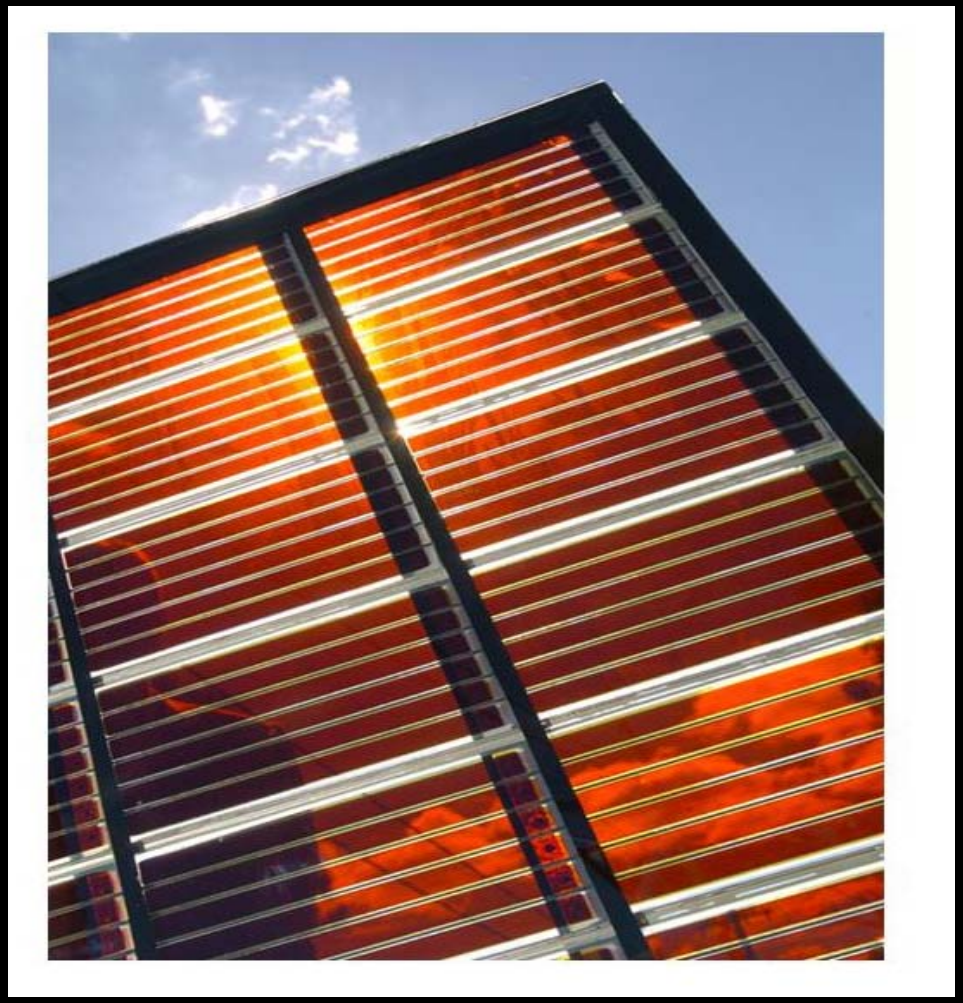

DYESOL-TATA (UK) / FUJIKURA (JPN)

From Design to Prototypes:

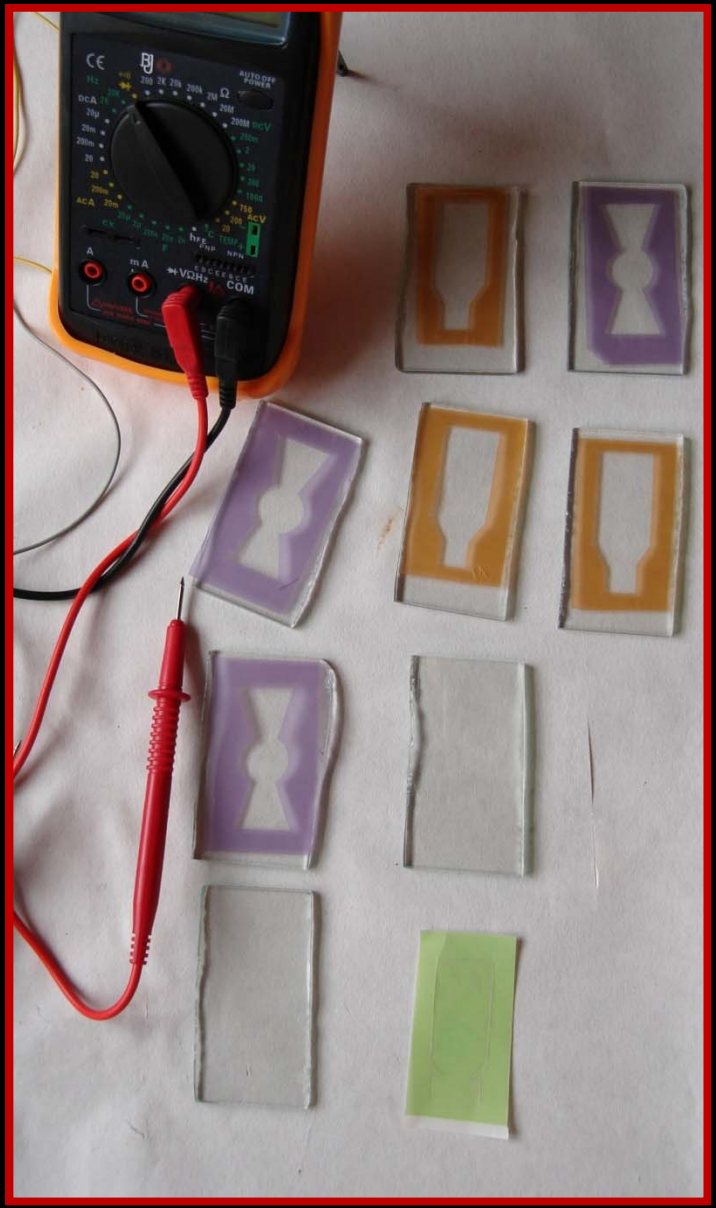

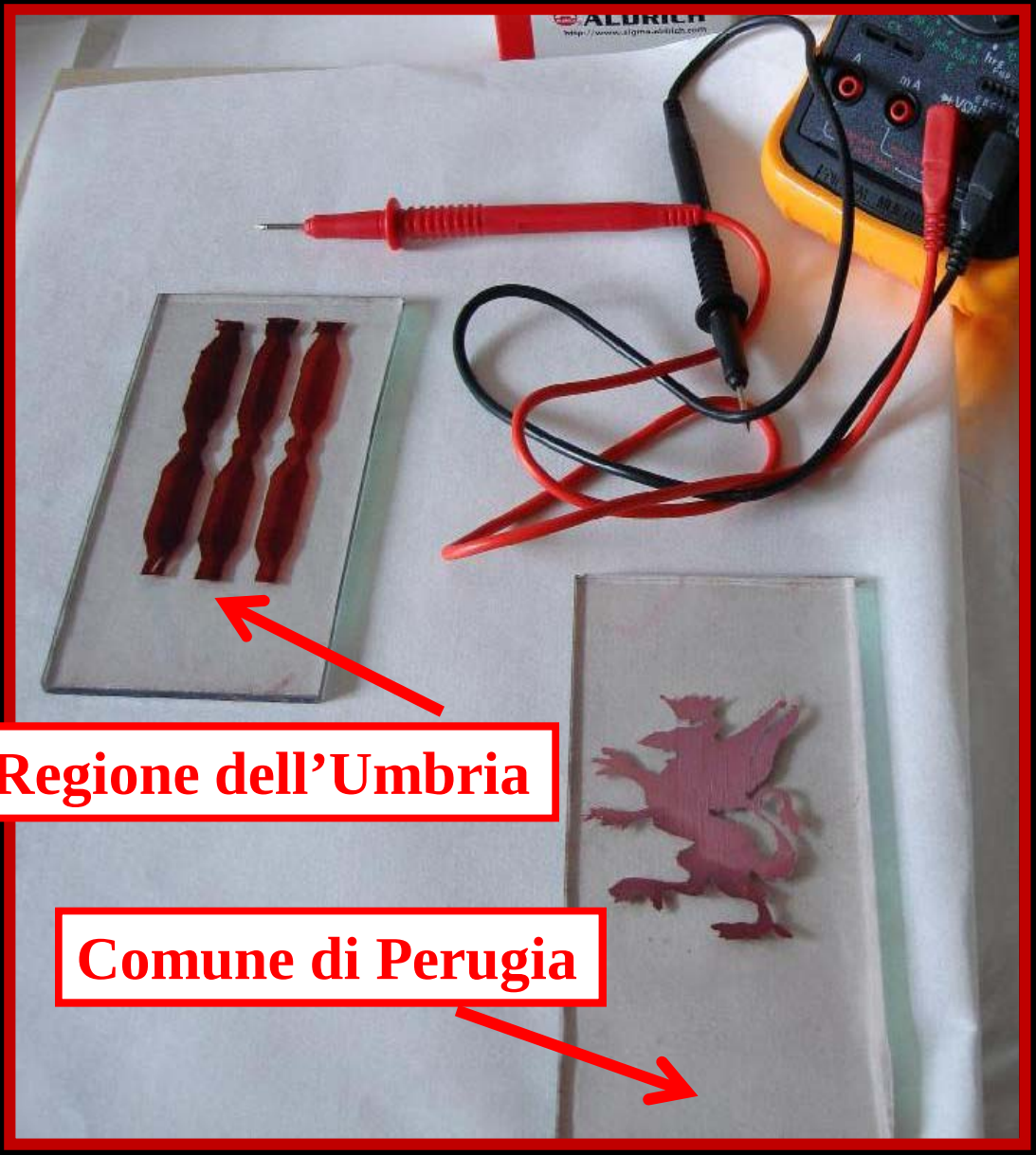

All materials purchased from Dyesol

Bulk heterjunction solar cells: $\eta > 7\ \%$

Polymer / fullerene blends

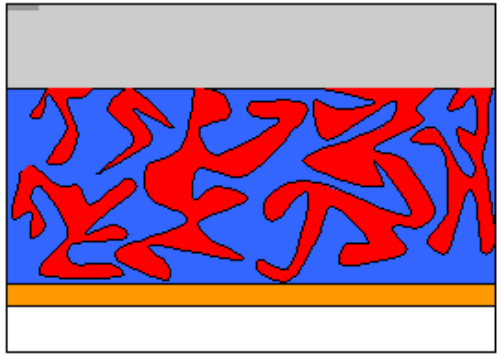

Bulk Heterojunction by Mixture

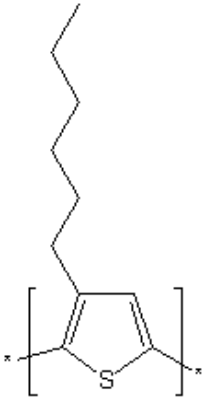

P3HT

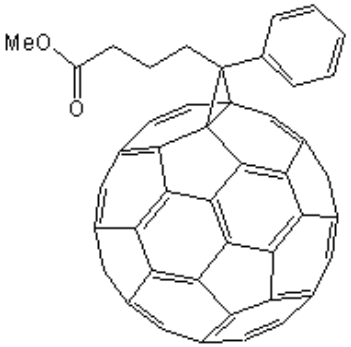

PCBM

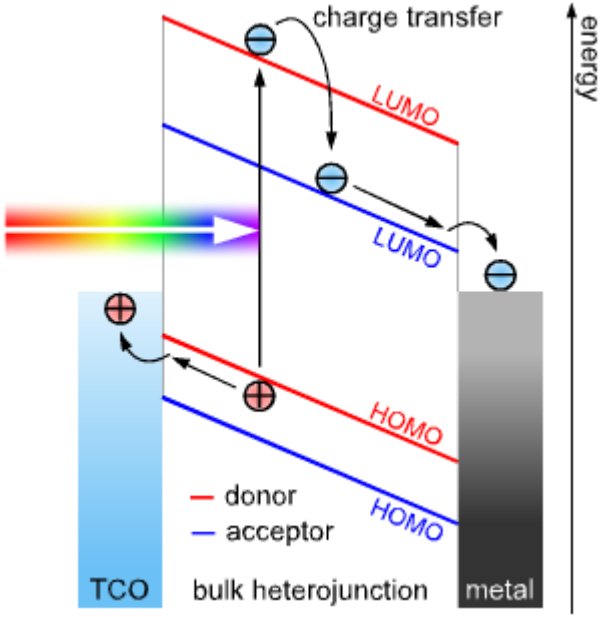

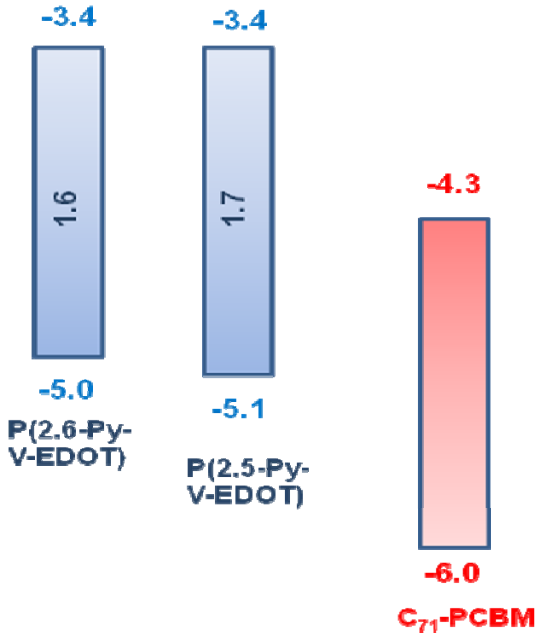

Part II
Modeling

The goal: modeling nanoscale devices

• **Large dimensions :** **realistic models usually require dealing with a few hundred atoms (oversimplified models are often inaccurate)**

•**Complexity :** **complex potential energy surfaces with several minima; dealing with transition metals (electronic correlation)**

•**Optical properties:** **need an accurate description of the excited states**

•**Dynamical aspects :** **need to perform ab initio molecular dynamics simulations**

Theoretical and computational approach

- Geometry optimizations of extended systems, in condensed phase, for both ground and excited states
- Ab initio molecular dynamics
- Calculation of absorption and emission spectra
- Inclusion of solvation effects (explicit or implicit models)

F. De Angelis, S. Fantacci, A. Sgamellotti, ***Theor. Chem. Acc.*** **2007, 17, 1093.**

The electronic Schrödinger equation:

Born-Oppenheimer approximation

$$\hat{H}_e \varphi_n(\mathbf{r};\mathbf{R}) = \varepsilon_n(\mathbf{R})\varphi_n(\mathbf{r};\mathbf{R})$$

The Hamiltonian for the electronic motion:

$$\hat{H}_e = -\tfrac{1}{2}\sum_i \nabla_i^2 - \sum_{a,i}\frac{Z_a}{r_{ai}} + \sum_{i>j}\frac{1}{r_{ij}} + \sum_{a>b}\frac{Z_a Z_b}{R_{ab}}$$

The electron-electron repulsion term makes it unsolvable for n>1

(SOB!!)

Evaluation of the energy and its derivatives:

•Quantum mechanics (ab initio)

•Multi-reference configuration interaction $\rightarrow N^{7-8}$ (MRCI)

•Coupled-cluster $\rightarrow N^{5-6}$ (CC)

•Density Functional Theory $\rightarrow N^{3-4}$ (DFT)

H_2O $\rightarrow$ 10 elettroni MRCI=30 min, CC=15 min, DFT=1 min

$2H_2O$ $\rightarrow$ 20 elettroni MRCI=7680(128 h) CC=960 (16h) DFT=8-16

•Semi-empirical methods

•INDO/MNDO/ZINDO $\rightarrow N^{2-3}$

•Model potentials

•force fields $\rightarrow N^{2}$

Dimensions/accuracy

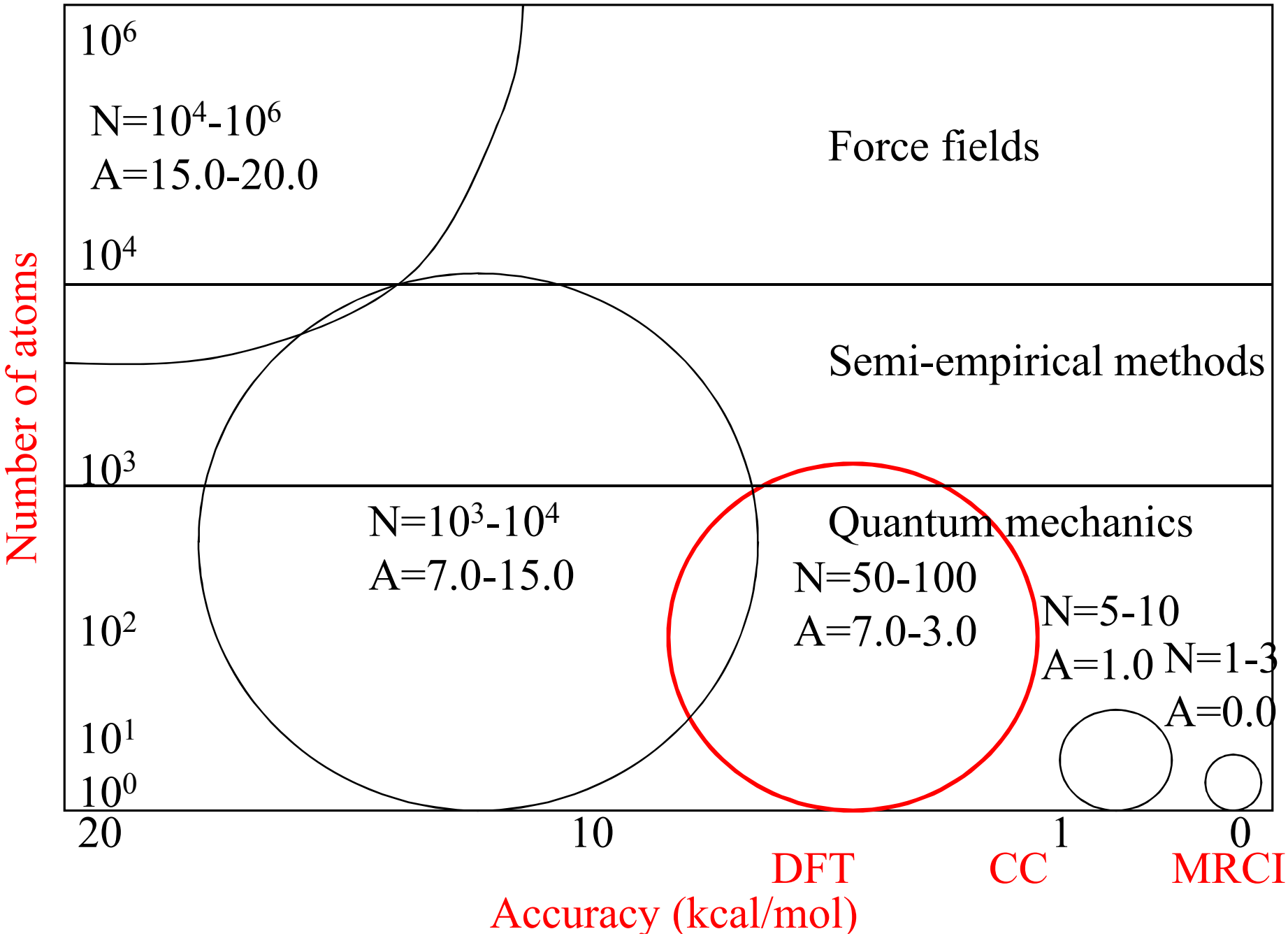

Density Functional Theory

- Hohenberg-Kohn theorems

$$E[\rho] = T_0[\rho] + J[\rho] + \int v(\mathbf{r})\,\rho(\mathbf{r})\,d\mathbf{r} + E_{\mathrm{xc}}[\rho]$$

The Energy is a Functional of the Electron Density

- Exchange-correlation potential

LDA, BP86, **<u>B3LYP</u>** PBE0

The unknown part of the electron-electron interaction

- Kohn-Sham equations

$$\left(-\frac{1}{2}\nabla^2 + V_S[\rho]\right)\varphi_i = \varepsilon_i\varphi_i \qquad \rho = \sum_i n_i |\phi_i|^2$$

Single particle equations (very simple to solve !!)

Potential Energy Surfaces (PES):

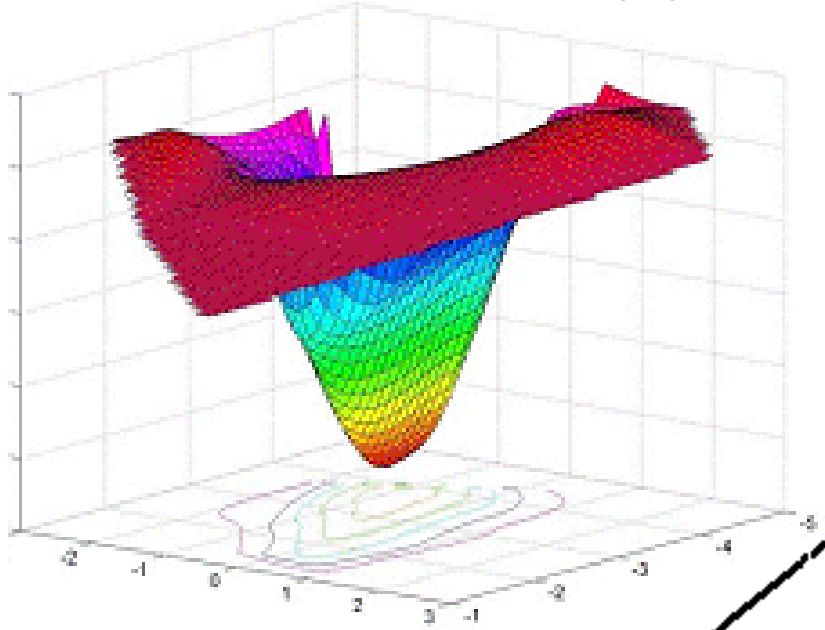

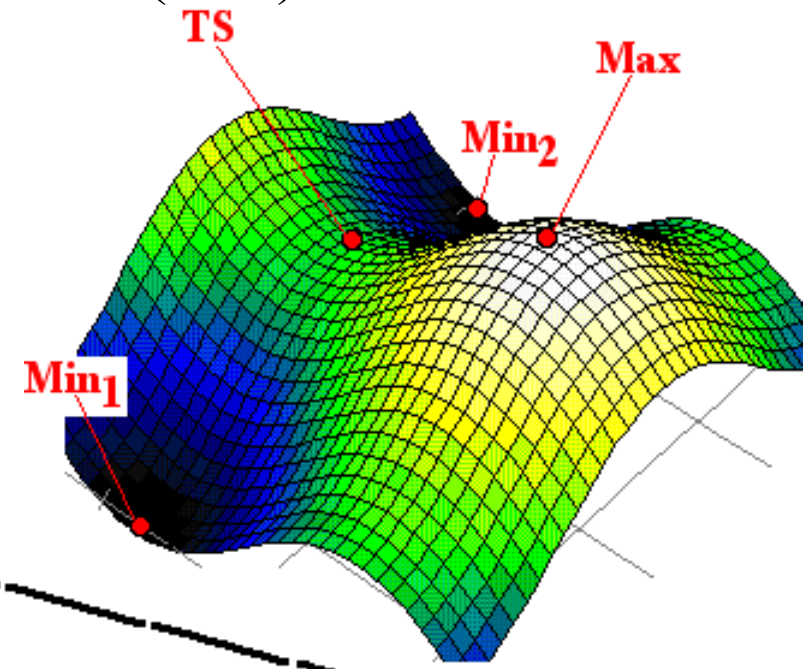

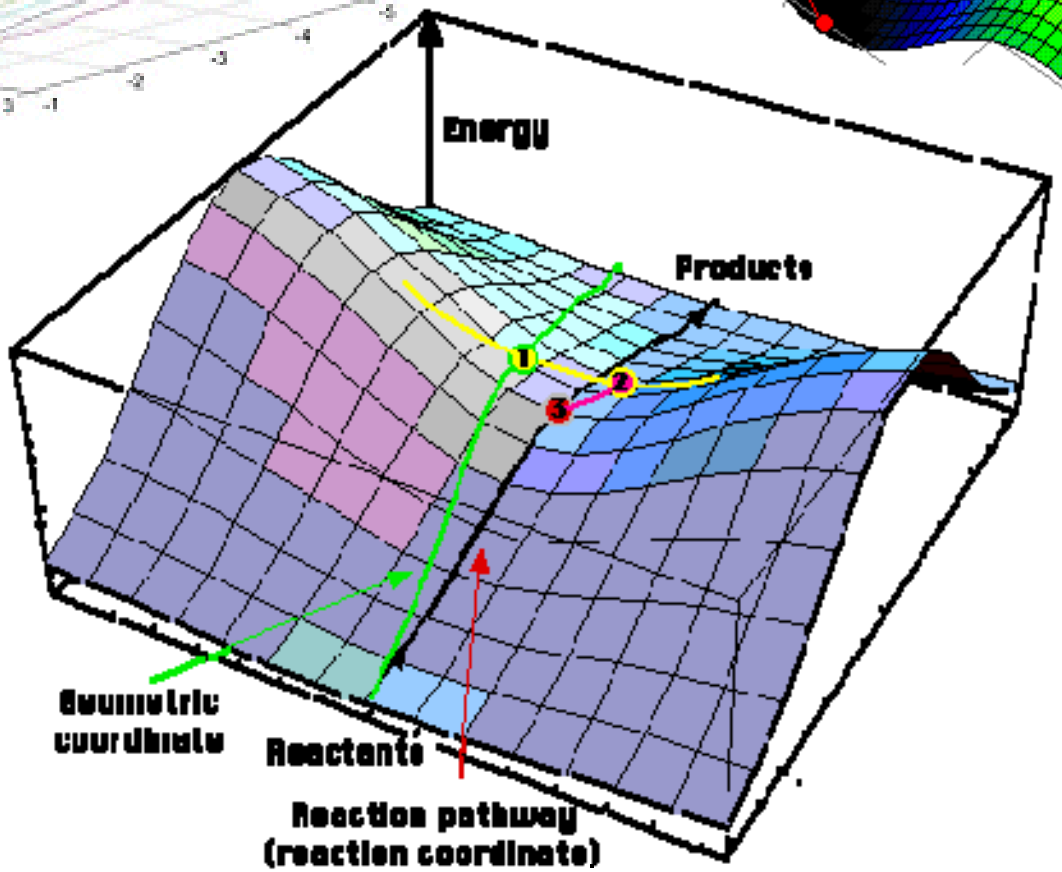

Gradient (first derivative) and Hessian (second derivative):

$$g(x) = \begin{bmatrix} \frac{\partial f}{\partial x_1} \\ \frac{\partial f}{\partial x_2} \\ \cdot \\ \cdot \\ \cdot \\ \frac{\partial f}{\partial x_n} \end{bmatrix} \qquad H(x) = \begin{bmatrix} \frac{\partial^2 f}{\partial x_1 \partial x_1} & \cdot & \cdot & \cdot & \frac{\partial^2 f}{\partial x_1 \partial x_n} \\ \cdot & \cdot & \cdot & \cdot & \cdot \\ \cdot & & & & \cdot \\ \cdot & & & & \cdot \\ \frac{\partial^2 f}{\partial x_n \partial x_1} & \cdot & \cdot & \cdot & \frac{\partial^2 f}{\partial x_n \partial x_n} \end{bmatrix}$$

Minima:

$$g(x) = \begin{bmatrix} \phi_1(x) \\ \phi_2(x) \\ \cdot \\ \cdot \\ \cdot \\ \phi_n(x) \end{bmatrix} \lambda(x) = \begin{bmatrix} \lambda_1(x) \\ \lambda_2(x) \\ \cdot \\ \cdot \\ \cdot \\ \lambda_n(x) \end{bmatrix}$$

Transition States:

$$g(x) = \begin{bmatrix} \phi_1(x) \\ \phi_2(x) \\ \cdot \\ \cdot \\ \cdot \\ \phi_n(x) \end{bmatrix} \lambda'(x) = \begin{bmatrix} -\lambda_1(x) \\ \lambda_2(x) \\ \cdot \\ \cdot \\ \cdot \\ \lambda_n(x) \end{bmatrix}$$

Gradient and Hessian matrices

First Principles Molecular Dynamics

We call *Molecular Dynamics* (MD) a computer simulation technique in which the time evolution of a set of interacting atoms is followed by integrating their equations of motion.

We limit our attention to a set of interacting atoms moving classically: the dynamics is described by Newton's law:

$$\boxed{\mathbf{F}_i = m_i \mathbf{a}_i}$$

$$\mathbf{a}_i = d^2\mathbf{r}_i/dt^2 \qquad \mathbf{F}_i \qquad \boldsymbol{m_i}$$

The interatomic potential:

$$\mathbf{F}_i = -\nabla_{\mathbf{r}_i} V(\mathbf{r}_1, \ldots, \mathbf{r}_N)$$

Born-Oppenheimer Molecular Dynamics (BOMD):

One could think of interfacing a standard quantum mechanics code (e.g. Gaussian03) to calculate the energy and its derivatives with a simple MD code to integrate the EOM.

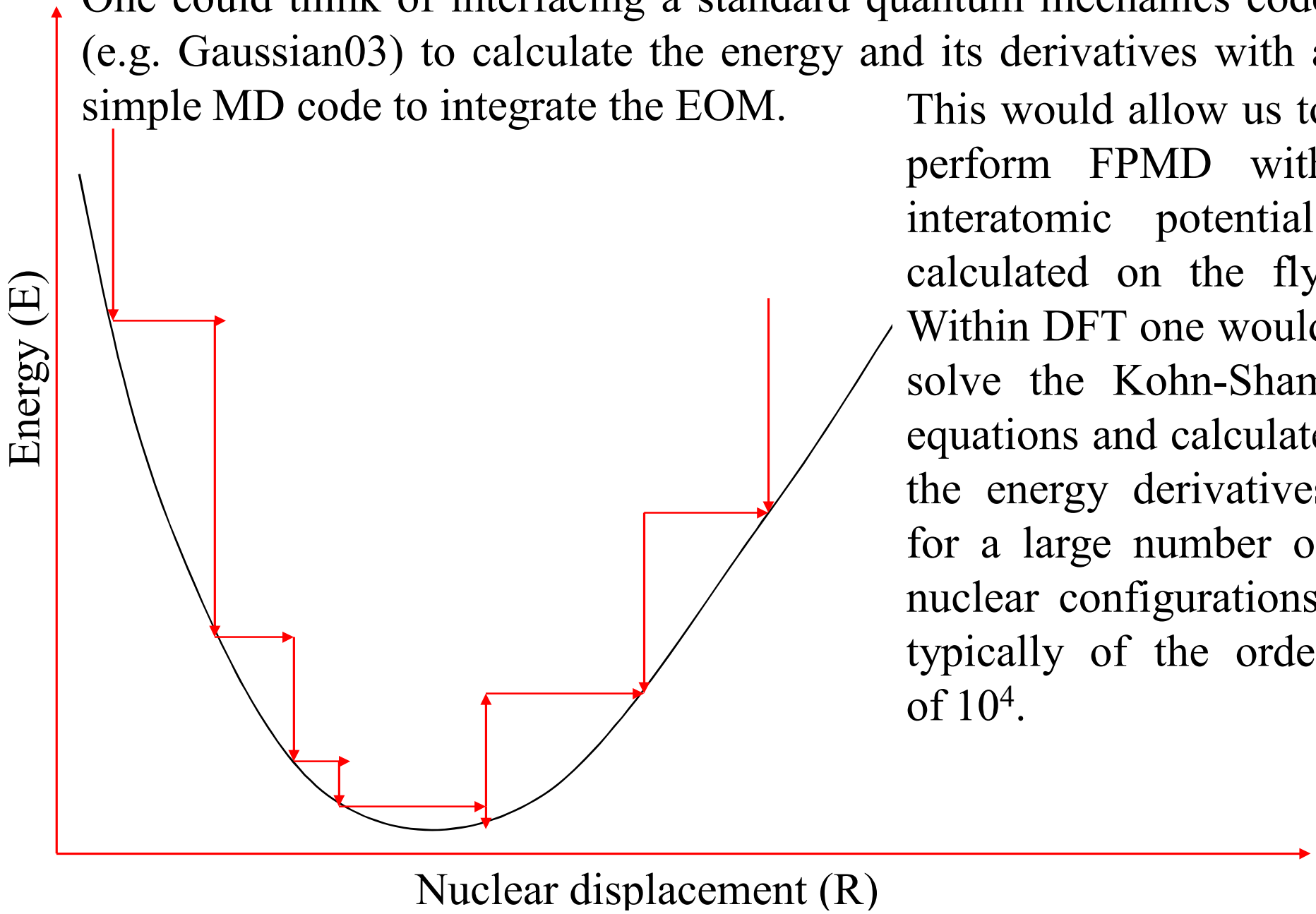

This would allow us to perform FPMD with interatomic potentials calculated on the fly. Within DFT one would solve the Kohn-Sham equations and calculate the energy derivatives for a large number of nuclear configurations, typically of the order of 10^4.

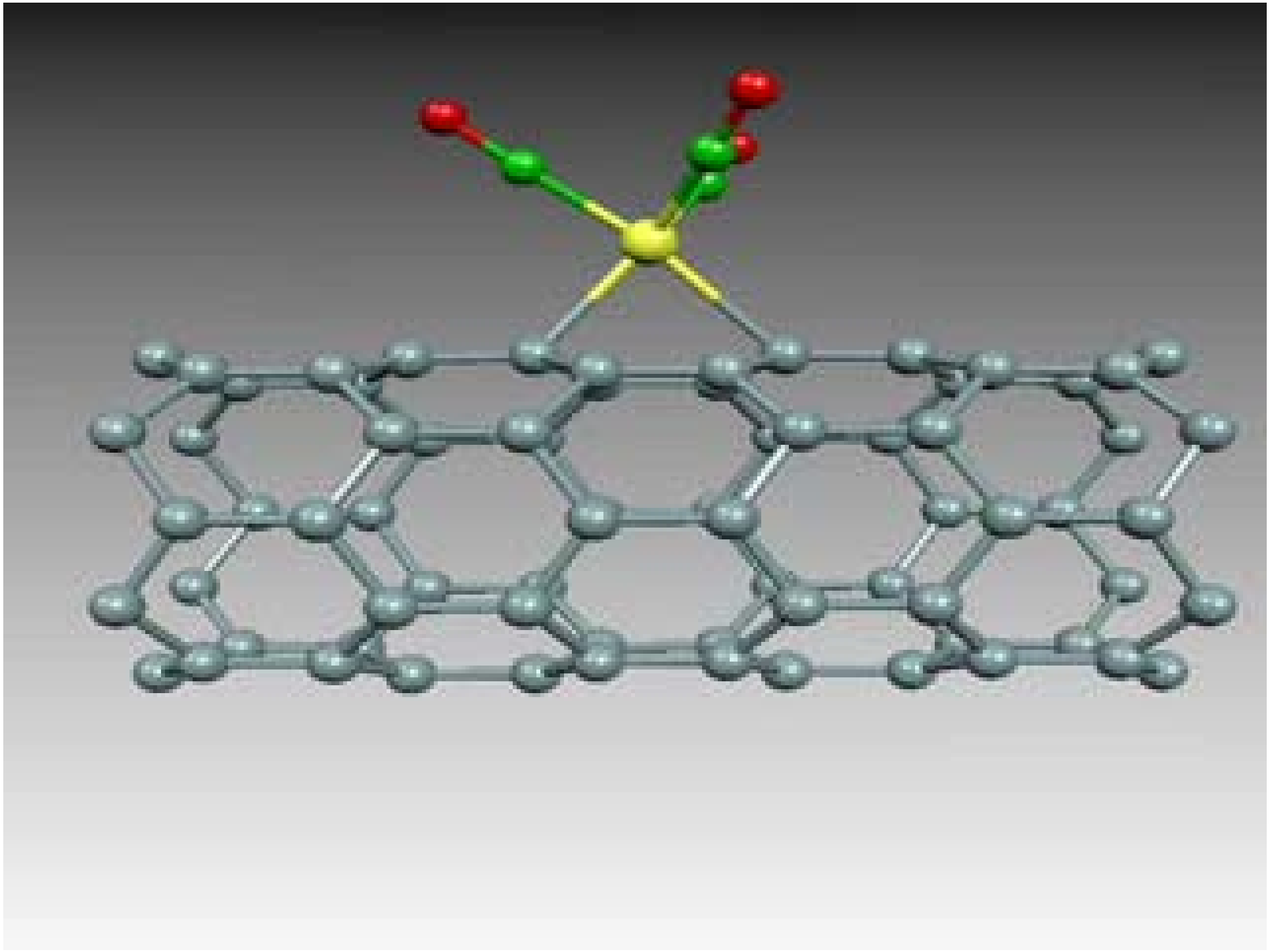

The Car-Parrinello method: DFT-based Molecular Dynamics

Generalized Lagrangian (nuclei + electrons)

$$L = \sum_i^{occ} \int dr\ \mu_i |\dot{\psi}_i(r)|^2 + \frac{1}{2} \sum_I M_I R_I^2 - E[\{R_I\}] + \sum_{ij} \Lambda_{ij} [\int dr \psi_i^*(r) \psi_j(r) - \delta_{ij}]$$

Classical equations of motion

$$\mu_i\ \dot{\Psi}_i(r,t) = -\frac{1}{2} \frac{\delta E}{\delta \Psi_i^*(r,t)}\ ; + \sum_j \Lambda_{ij} \Psi_j$$

$$M_I\ \ddot{R}_I = -\frac{\Delta E}{\Delta R_I}$$

Plane-Wave basis set

$$\psi_i^k(r) = e^{ik*r} \sum_g c_i^k(g)\ e^{ik*r}$$

Kinetic Energy

$$E_{\text{kin}} = \frac{1}{2} \sum_{i,\mathbf{G}}^{\mathbf{G}_c^{\text{wf}}} G^2 |\phi_i(\mathbf{G})|^2$$

FFT → PP's

Hartree Potential

$$E_H = 2\pi\Omega \sum_{\mathbf{G}\neq 0}^{\mathbf{G}_c^{\text{dens}}} \frac{n^*(\mathbf{G}) n(\mathbf{G})}{G^2}$$

Car-Parrinello Molecular Dynamics (CPMD)

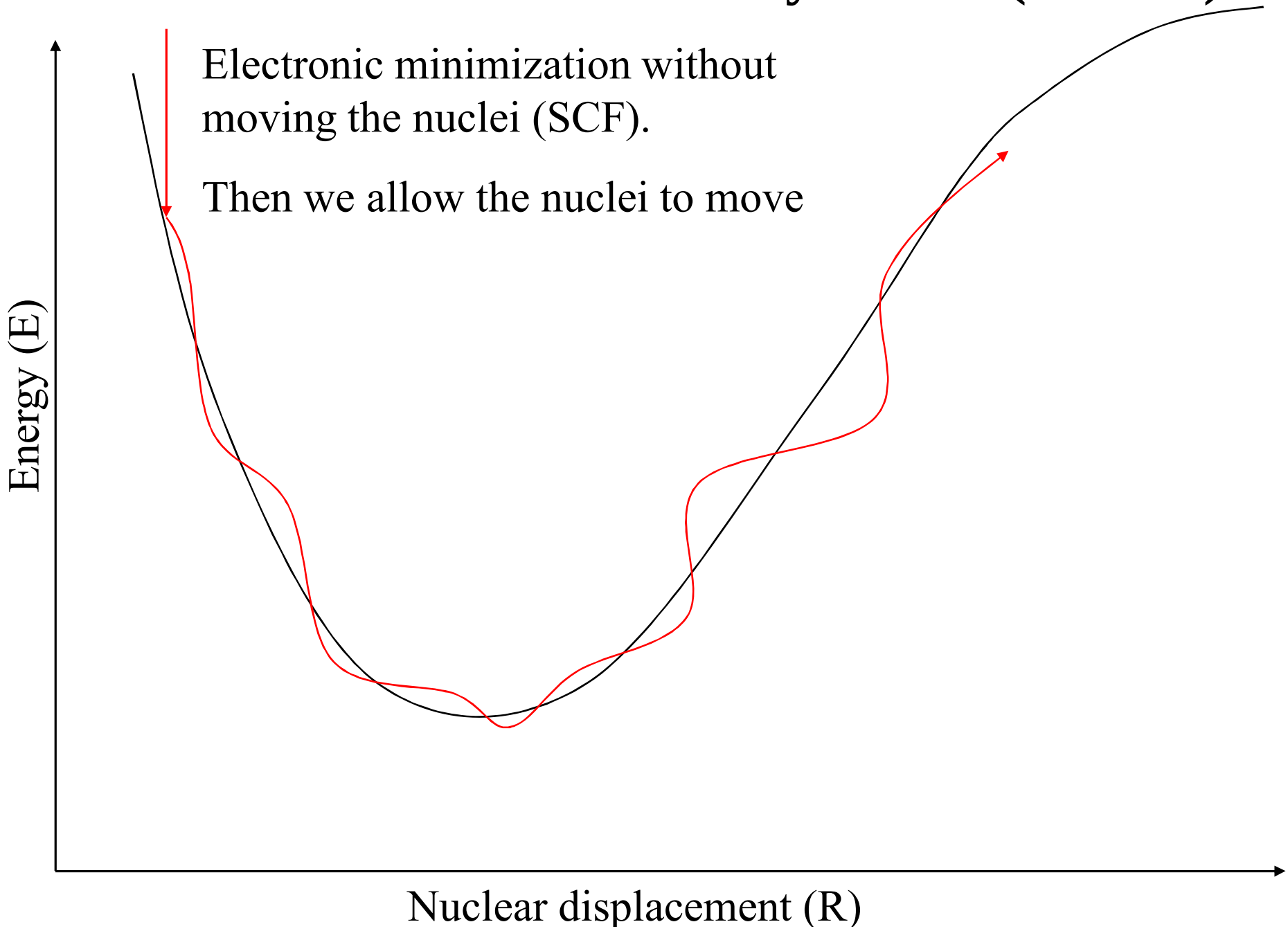

Vanderbilt Pseudopotentials:

Partition of the electron density into soft (delocalized) and hard (localized) terms

$$n(\mathbf{r}) = \sum_i \left[\, |\phi_i(\mathbf{r})|^2 + \sum_{nm,I} Q^I_{nm}(\mathbf{r}) \langle \phi_i | \beta^I_n \rangle \langle \beta^I_m | \phi_i \rangle \, \right]$$

Double FFT grid techniques:

Calculation of delocalized terms in reciprocal space

Real space integrals localized in the core region

<u>Reduction of the computational cost by a factor 2-4</u>

Highly efficient parallelization:

P. Giannozzi, F. De Angelis, R. Car

J. Chem. Phys. 120, **2004**, 5903.

Solute-solvent interactions (PCM):

F. De Angelis, M. Cossi, V. Barone *et al.*

Chem. Phys. Lett. 328, **2000**, 302

Bio-inorganic chemistry:

F. De Angelis, R. Car, T.G. Spiro

J. Am. Chem. Soc. 125, **2003**, 15710.

Organometallic reactivity:

F. De Angelis, S. Fantacci, A. Sgamellotti

Coord. Chem. Rev. 250, **2006**, 1497.

Excited states:Time Dependent DFT

- Time Dependent Kohn-Sham Method

$$\left(-\frac{1}{2}\nabla^2 + V_S[\rho(t)]\right)\varphi_i(t) = i\frac{\partial\varphi_i(t)}{\partial t} \qquad \rho(t) = \sum_i n_i |\phi_i(t)|^2$$

- Adiabatic Local Density Approximation (ALDA)

$\delta\ v_{xc}[\rho](r,t)\ /\ \delta\ \rho(r',t') \approx \delta\ v_{xc}[\rho_t](r)\ /\ \delta\ \rho_t(r')$

- Calculation of transition energies and oscillator strengths absorption and emission spectra, NLO properties (2n+1 theorem and/or SOS)

• The excited state density is expressed as a linear combination of single occupied to virtual orbital excitations

$$\mathbf{ES} = \sum_i \mathbf{c_i}\,(\,\mathbf{o\ o'|\ vv'}\,)$$

Continuum solvation models:

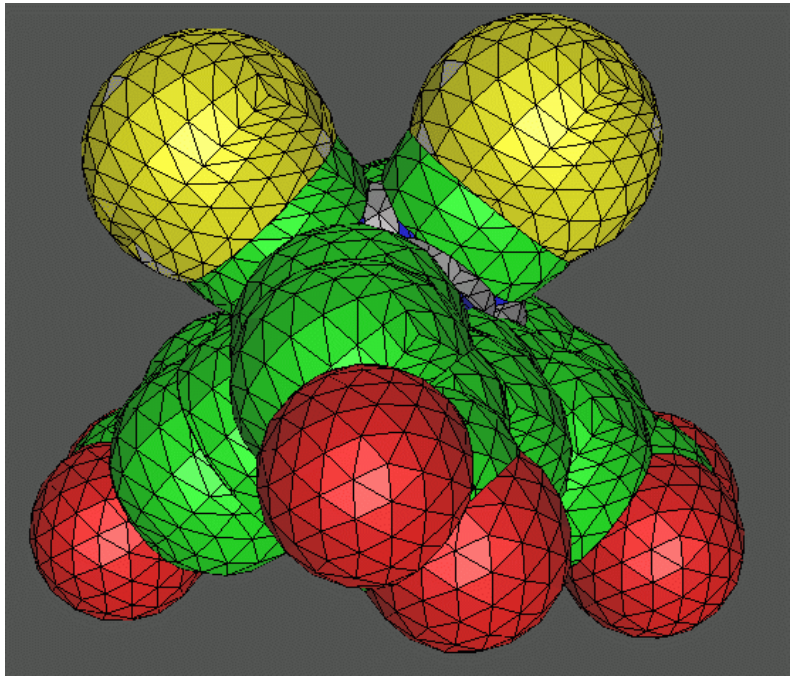

$$\varepsilon(r) = \begin{cases} 1 \text{ inside} \\ \varepsilon \text{ outside} \end{cases}$$

Solvent response by apparent surface charges:

$$\hat{\mathcal{V}}_\sigma(\vec{r}) = \sum_i^{tesserae} \frac{q_i}{|r - r_i|}$$

Solvation effects in TDDFT:

$$\begin{pmatrix} \mathbf{A} & \mathbf{B} \\ \mathbf{B}^* & \mathbf{A}^* \end{pmatrix} \begin{pmatrix} \mathbf{X}_n \\ \mathbf{Y}_n \end{pmatrix} = \omega_n \begin{pmatrix} 1 & 0 \\ 0 & -1 \end{pmatrix} \begin{pmatrix} \mathbf{X}_n \\ \mathbf{Y}_n \end{pmatrix}$$

Pseudo-eigenvalue problem

$$A_{ai,bj} = \delta_{ab}\delta_{ij}(\epsilon_a - \epsilon_i) + K_{ai,bj} + \boxed{\mathcal{B}^{IEF}_{ai,bj}}$$

$$B_{ai,bj} = +K_{ai,jb} + \boxed{\mathcal{B}^{IEF}_{ai,bj}}$$

Coupling matrices

$$K_{ai,bj} = \int d\mathbf{r} \int d\mathbf{r}' \phi_i(\mathbf{r}')\, \phi_a{}^*(\mathbf{r}') \left(\frac{1}{|\mathbf{r}' - \mathbf{r}|} + g_{xc}(\mathbf{r}', \mathbf{r}) \right) \phi_j(\mathbf{r})\, \phi_b{}^*(\mathbf{r})$$

$$\boxed{\mathcal{B}^{IEF}_{ai,bj} = \sum_k \left(\int d\mathbf{r}\, \phi_i(\mathbf{r}')\, \phi_a{}^*(\mathbf{r}') \frac{1}{|\mathbf{r}' - \mathbf{s}_k|} \right) q(\mathbf{s}_k; \epsilon_\omega, \phi_j \phi_b{}^*)}$$

Coupling matrix elements

M. Cossi, V. Barone *J. Chem. Phys.*, **2001**, *115*, 4708

Molecular dynamics of a TiO2-adsorbed dye in water

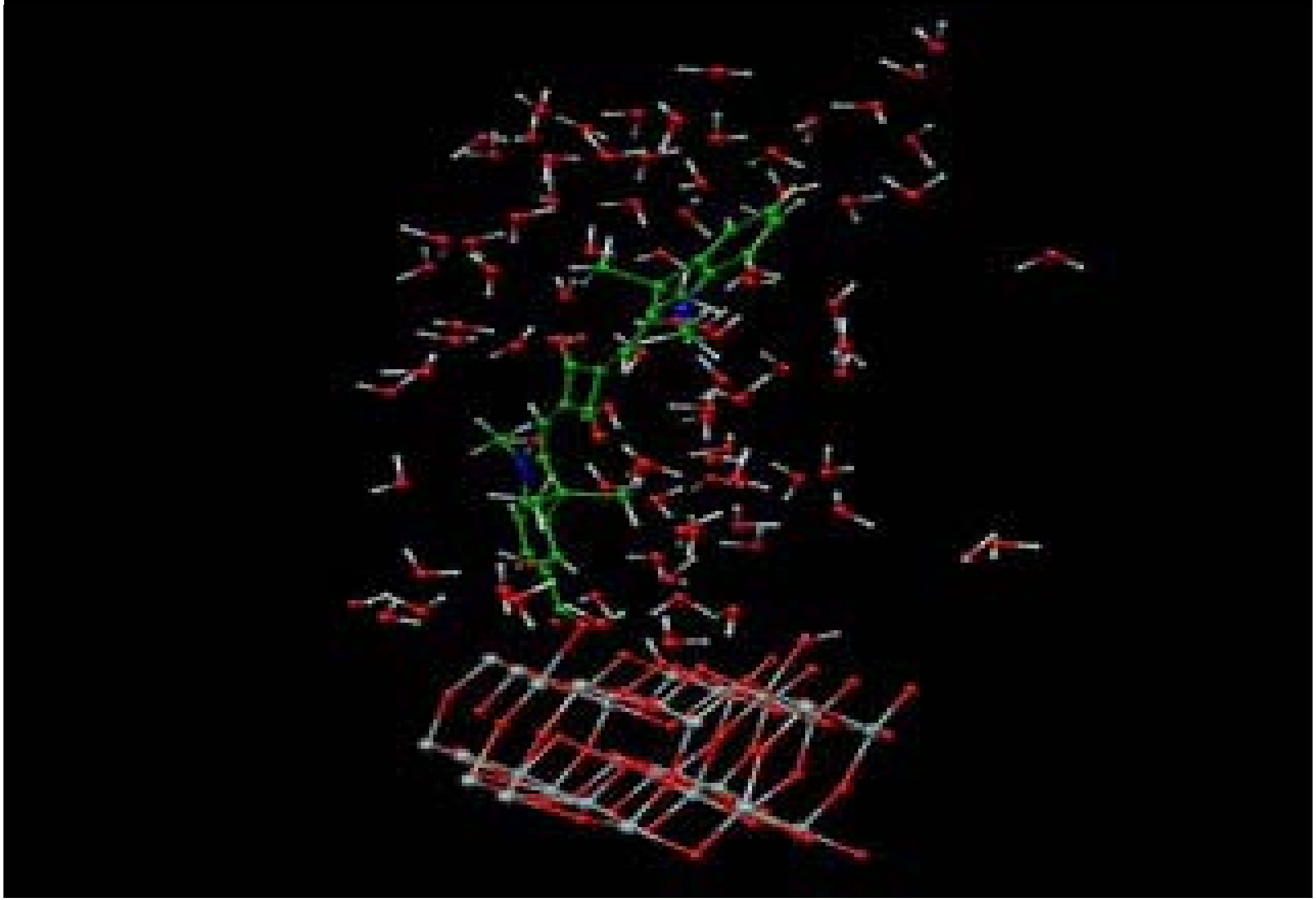

Computer Codes:

• GAUSSIAN 09	- USA
• TURBOMOLE	- GERMANY
• MOLPRO	- GERMANY
• GAMESS	- UK / USA
• ADF	- NETHERLANDS
• QUANTUM ESPRESSO	- ITALY
• ABINIT	- BELGIUM
•CP2K	- SWITZERLAND

COMPUTER RESOURCES

COMPUTER POWER: MOORE's LAW

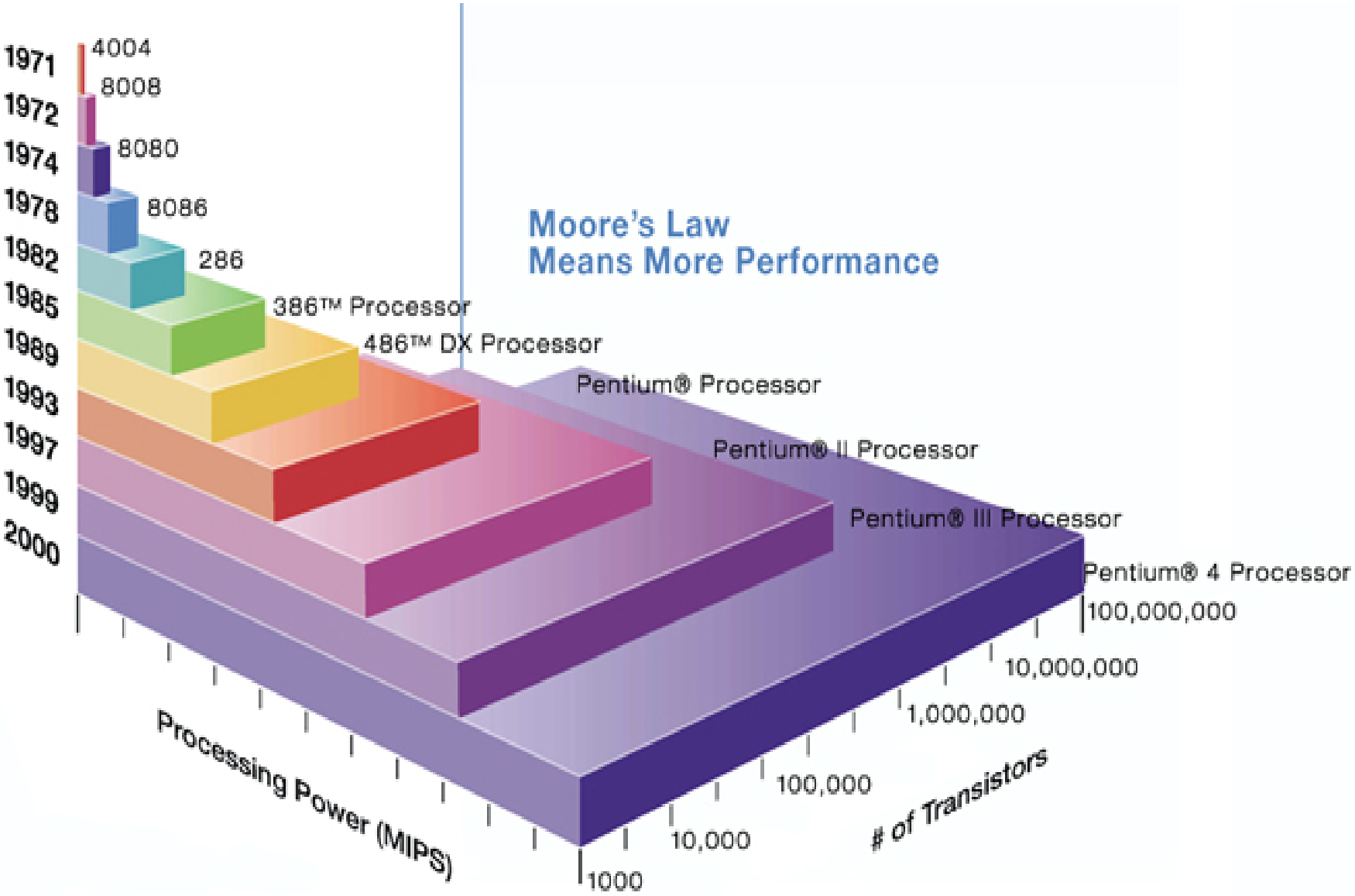

Computer power doubles every 18 months!!!

Part III
Results

Dye-sensitized solar cells: η=11.3 %

Ru(II)-polypyridyl sensitizers on TiO_2

$$\eta = i_{ph}\, V_{oc}\, ff / I_s$$

i_{ph} → rate of electron injection

V_{oc} → position of the conduction band

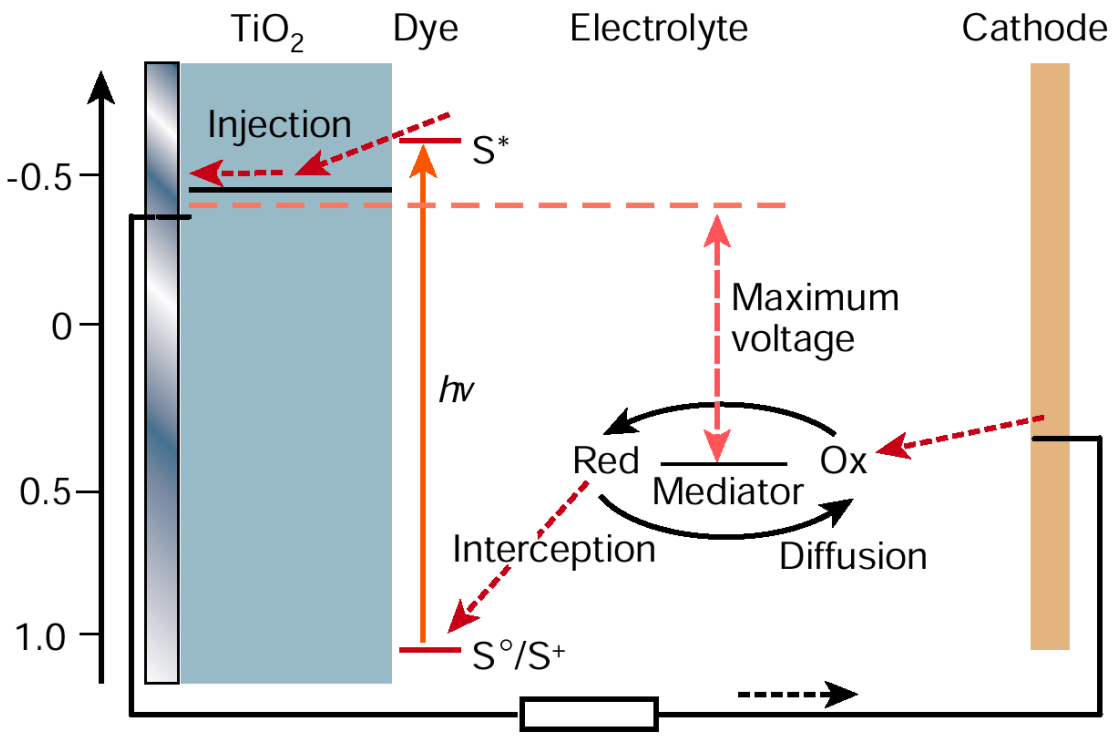

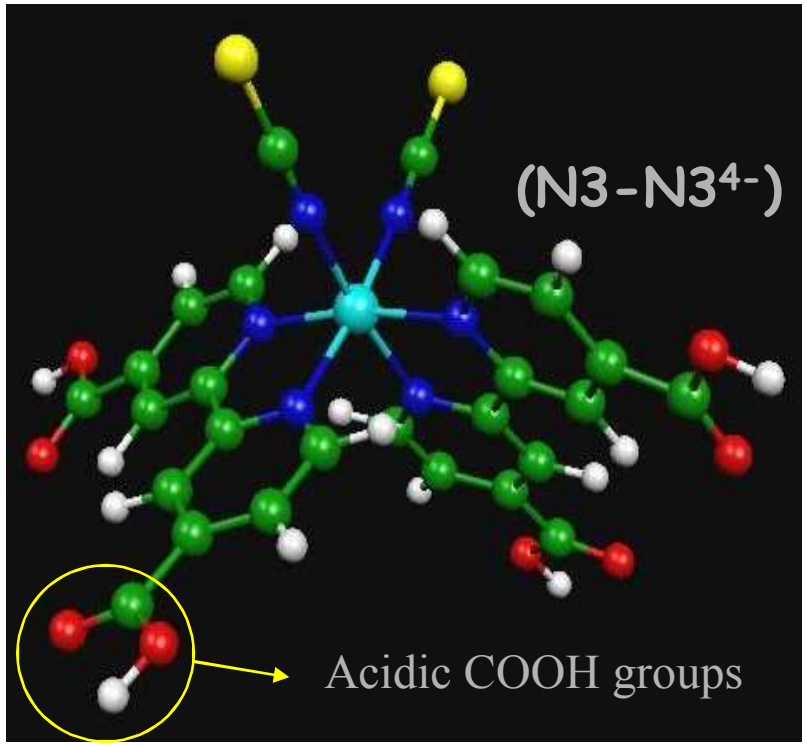

Indirect injection mechanism →No changes in free and adsorbed absorption spectra

O'Regan, B.; Grätzel, M. *Nature*, **1991**, *353*, 737 ; M. Grätzel, *Nature*, **2001**, 414, 338.

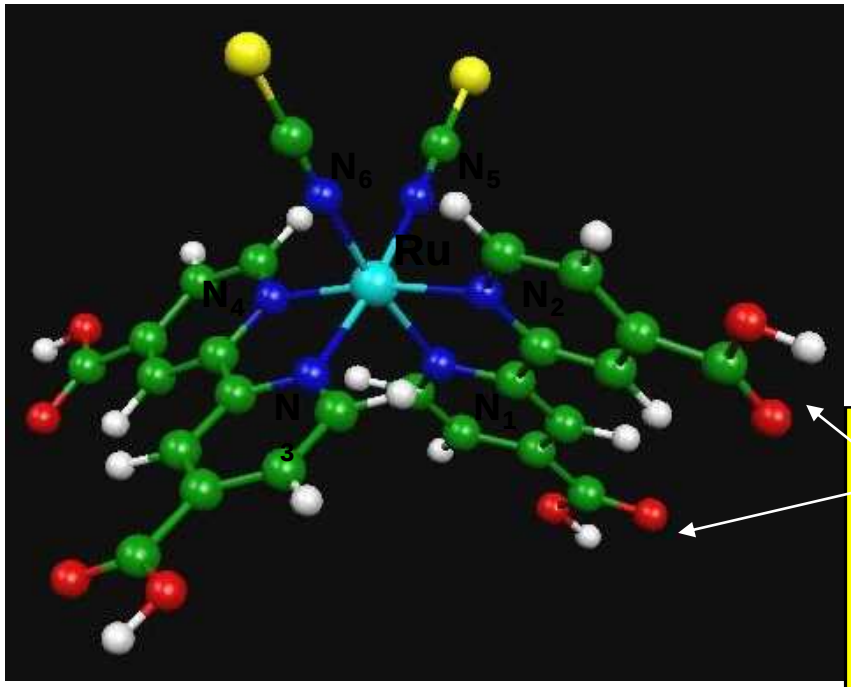

The N3 dye:

Ru(II) d^6 electron configuration. Singlet ground state. The triplet and quintet lie 14 e 41 kcal/mol higher in energy.

The terminal carboxylic groups can be either protonated or deprotonoated and allow stable anchoring of the dye to the TiO_2 surface

Calculated and experimental geometrical parameters

	Ru-$N_{1,3}$	Ru-$N_{2,4}$	Ru-$N_{5,6}$	N_1RuN_2	N_1RuN_3	N_1RuN_4	N_2RuN_4	N_5RuN_6
Exp.	2.036 2.058	2.030 2.013	2.048 2.046	79.8(5) 79.1(5)	90.6(5)	97.8(5) 95.9(5)	174.5(6)	88.2(5)
Theor.	2.079	2.056	2.036	78.9	95.1	94.0	169.5	90.2

S. Fantacci, F. De Angelis, A. Selloni ***J. Am. Chem. Soc.*** **2003, *125*, 4381.**

Analysis of the electronic structure:

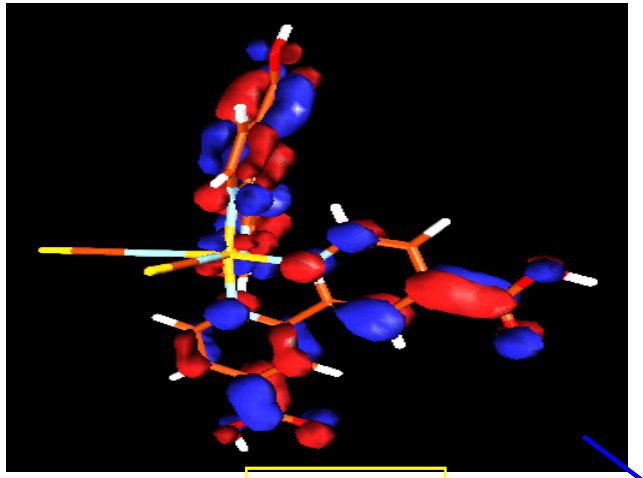

LUMO

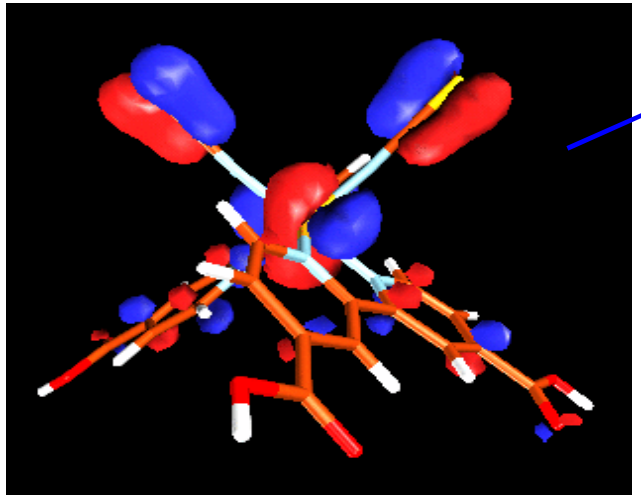

HOMO

MO	occ.	E(eV)	Ru	dcbpy	NCS
60a	0	-3.58		84(C); 4(O)	
59b	0	-3.73		87(C)	
59a	0	-3.92	4(d_{z^2})	59(C); 15(N); 12(O)	
58b	0	-3.94	3(d_{yz})	67(C); 14(N); 13(O)	
58a	0	-4.35	7(d_{z^2})	44(C); 21(N); 5(O)	
57b	0	-4.51	7(d_{yz})	47(C); 23(N); 7(O)	
57a	2	-4.95	10(d_{xy}); 6(d_{z^2})		55(S); 18(N)
56b	2	-5.08	10(d_{yz})		49(S); 20(N)
56a	2	-5.10	3(d_{xy}); 2(d_{z^2}); 2($d_{x^2-y^2}$)		59(S); 20(N)
55b	2	-5.19			69(S); 25(N)
55a	2	-6.53	45(d_{xy}); 16(d_{z^2})		19(S); 11(C)
54b	2	-6.57	59(d_{yz})		14(S); 15(C)
54a	2	-6.73	24(d_{z^2}); 18($d_{x^2-y^2}$); 14(d_{xy})		15(S); 21(C)

S. Fantacci, F. De Angelis, A. Selloni ***J. Am. Chem. Soc.*** **2003, *125*, 4381.**

Analysis of the excited states:

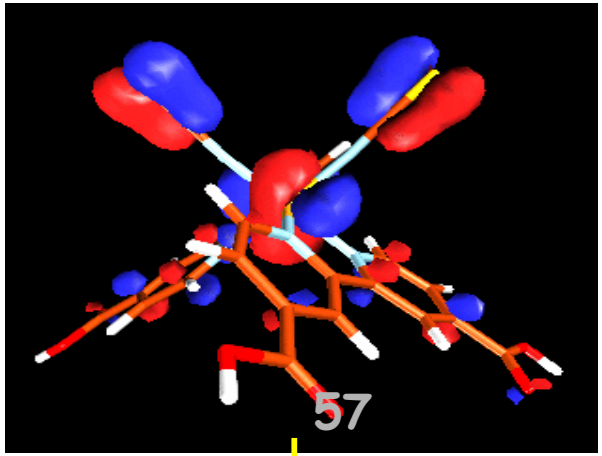

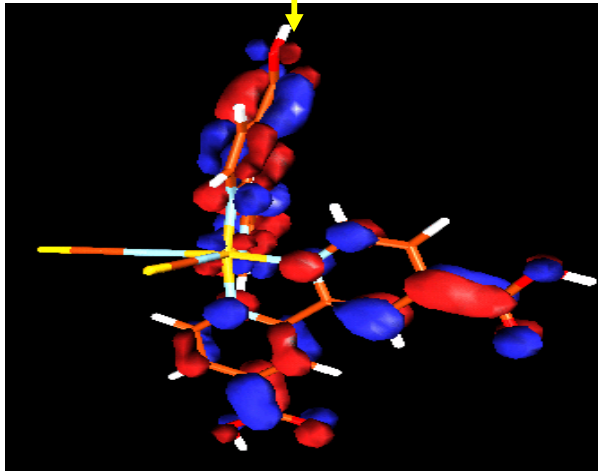

state	composition	E(eV)	f
3 ^{1}B	51%(56b→58a); 19%(55b→58a); 13%(57a→58b); 13%(56a→57b)	0.901	0.019
4 ^{1}B	65%(55b→58a); 15%(56b→58a); 7%(55b→59a); 6%(56a→58b)	0.994	0.012
5 ^{1}B	81%(57a→58b); 9%(56b→58a)	1.094	0.024
8 ^{1}B	46%(57a→59b), 20%(56b→59a); 19%(56a→58b); 13%(55b→59a)	1.257	0.0166
8 ^{1}A	40%(57a→60a); 38%(56b→59b); 6%(56a→59a)	1.357	0.0177
9 ^{1}A	53%(56b→59b); 22%(57a→60a); 10%(56b→58b);	1.379	0.0164
10 ^{1}B	58%(55b→59a); 17%(56a→58b); 7%(56b→60a)	1.430	0.0814
10 ^{1}A	28%(57a→60a); 20%(55b→59b); 13%(57a→59a);	1.445	0.0794
	10%(56a→59a); 9%(56a→60a)		
11 ^{1}A	79%(55b→59b); 8%(57a→59a)	1.472	0.0337
11 ^{1}B	92%(56b→60a)	1.515	0.0163
12 ^{1}A	89%(56a→60a)	1.534	0.0253

Solvatochromism:

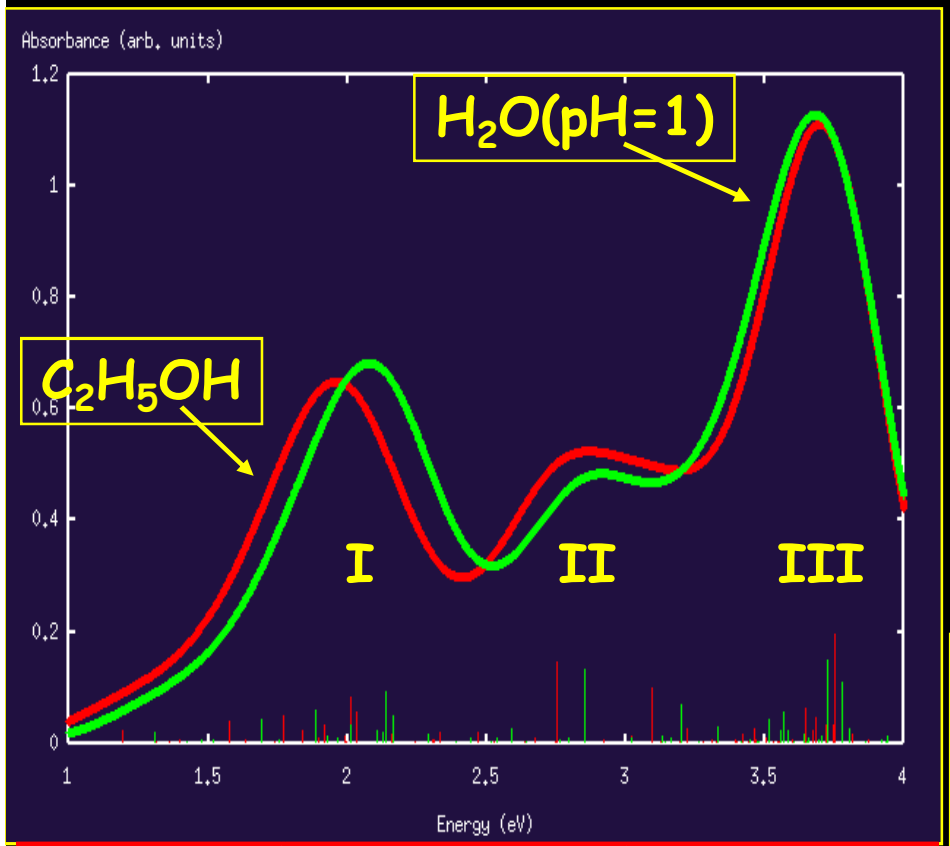

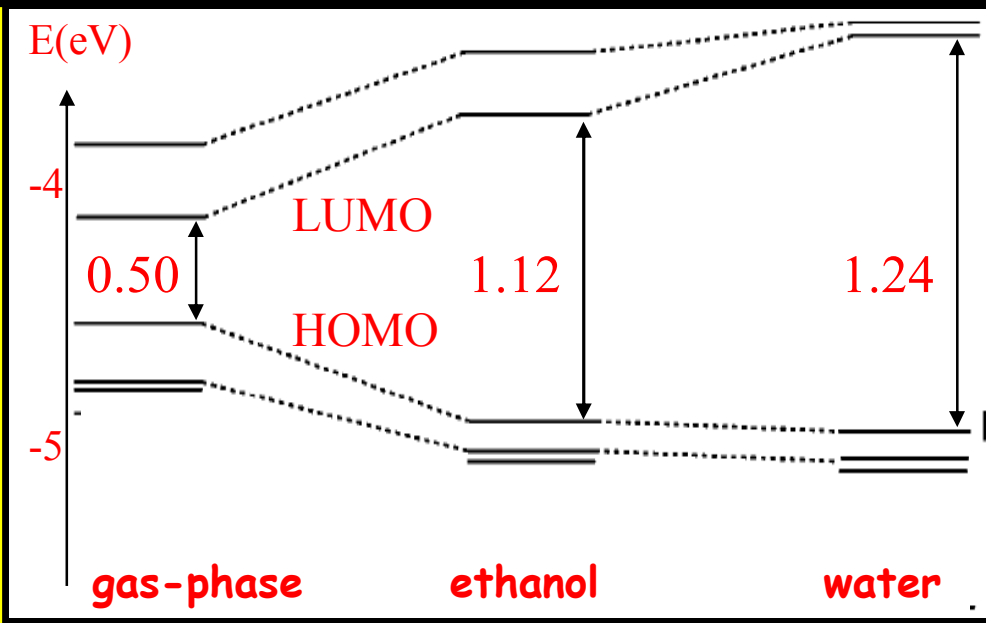

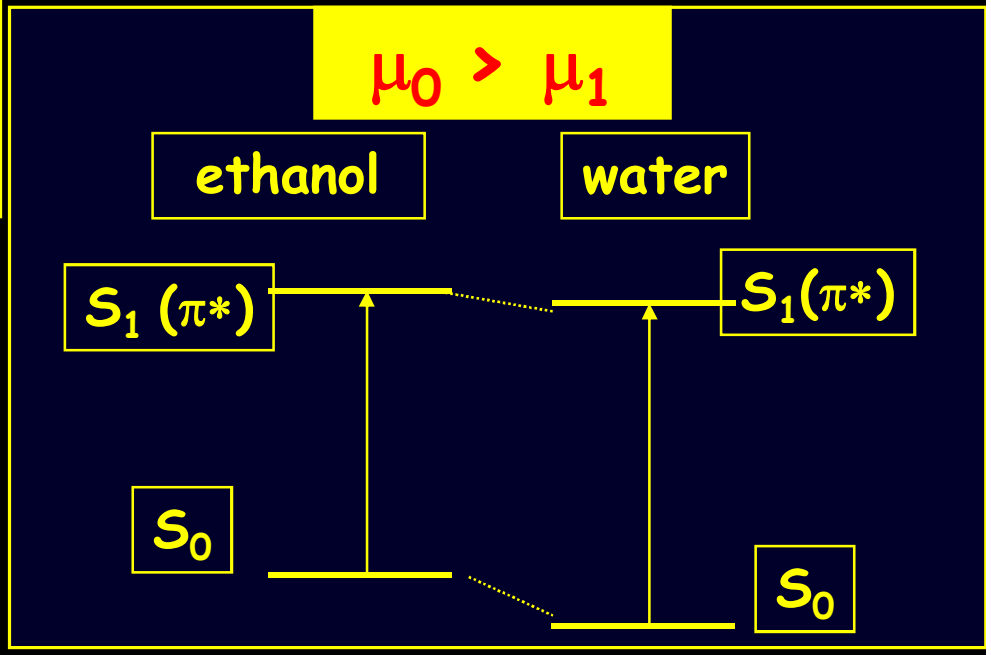

	Experimental (eV)			$\Delta E_{(I-II)}$	$\Delta E_{(II-III)}$
C_2H_5OH	2.30	3.12	3.95	0.82	0.83
H_2O (pH = 1)	2.38	3.18	3.97	0.80	0.79
$\Delta E_{C_2H_5OH/H_2O}$[b]	0.08	0.06	0.02		
	ALDA/BPW91 (eV)			$\Delta E_{(I-II)}$	$\Delta E_{(II-III)}$
C_2H_5OH	1.97	2.86	3.70	0.89	0.84
H_2O	2.08	2.92	3.69	0.84	0.77
$\Delta E_{C_2H_5OH/H_2O}$	0.11	0.06	0.01		

S. Fantacci, F. De Angelis, A. Selloni ***J. Am. Chem. Soc.*** **2003, *125*, 4381.**

Absorption spectrum of N719 in water:

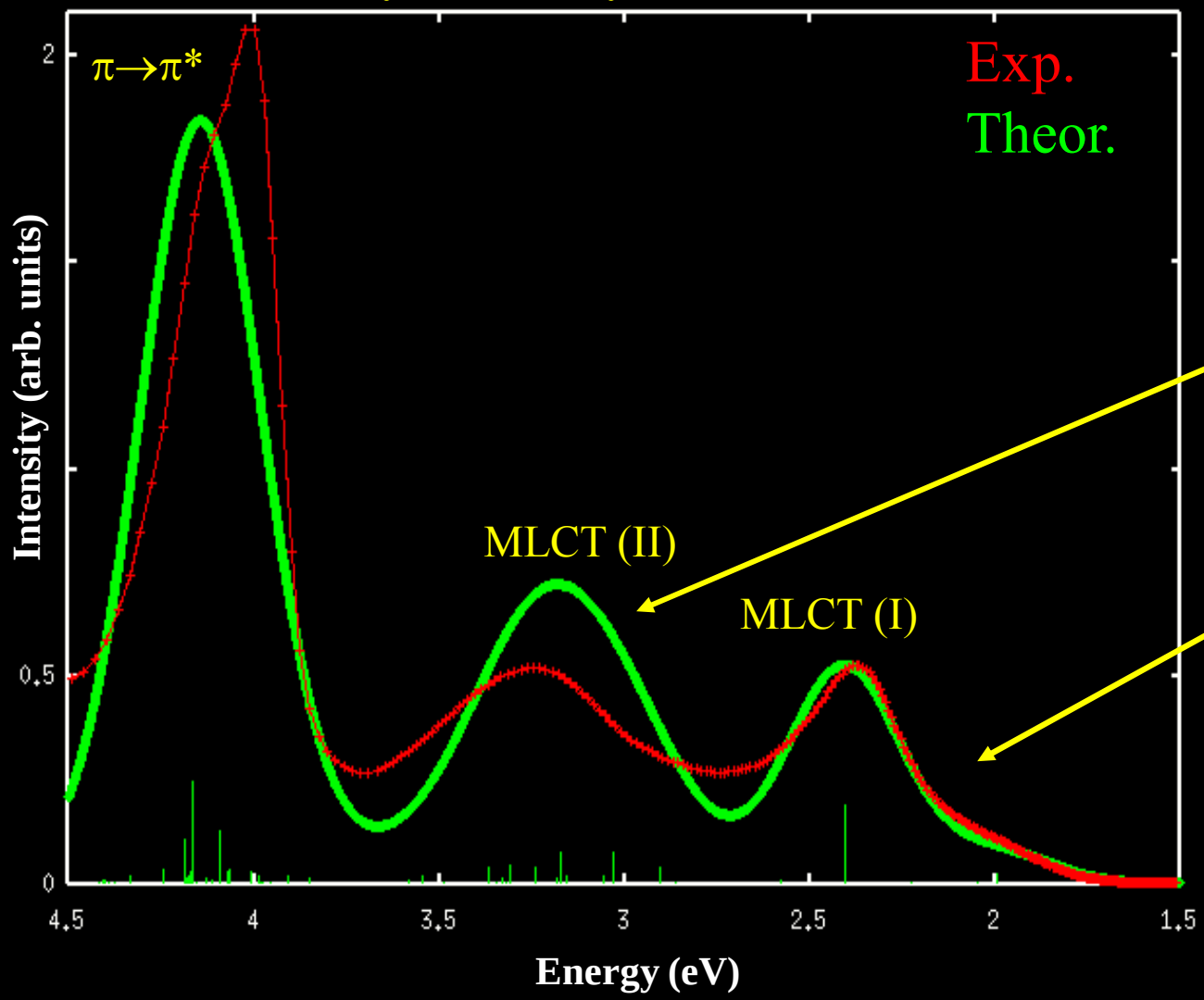

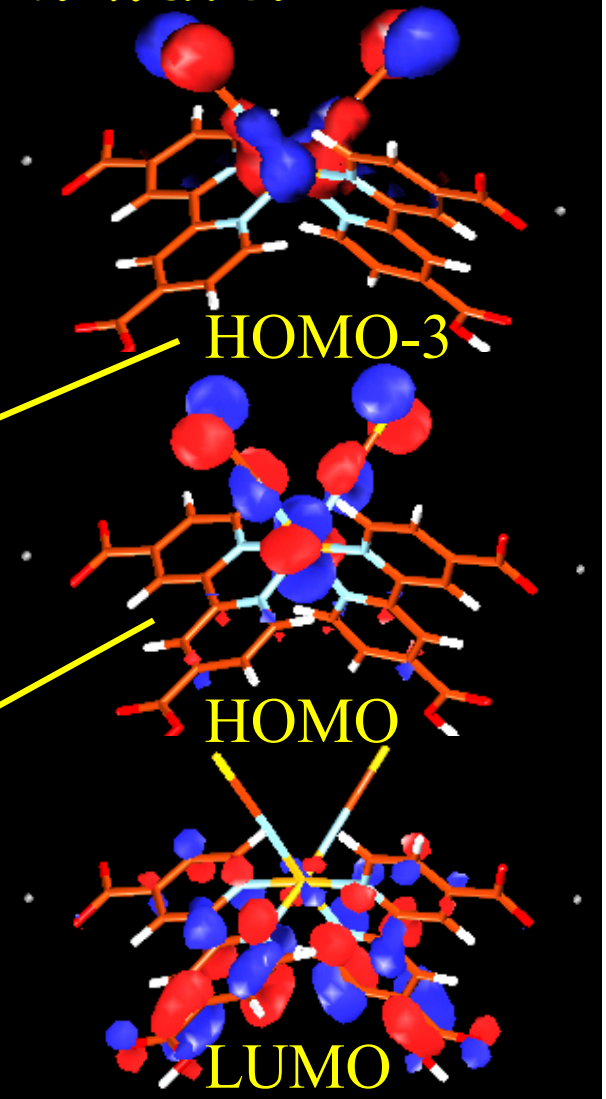

S. Fantacci, F. De Angelis, A. Selloni — ***J. Am. Chem. Soc.*** **2003, *125*, 4381.**
F. De Angelis, S. Fantacci, A. Selloni — ***Chem. Phys. Lett.*** **2004, *389*, 204.**
F. De Angelis, S. Fantacci, M.K. Nazeeruddin — ***Chem. Phys. Lett.*** **2005, *415*, 115.**
F. De Angelis,. S. Fantacci, M. Grätzel et al. — ***J. Am. Chem. Soc.*** **2005, *127*, 16835.**

Pyridine-EDOT Heteroarylene-Vinylene Donor-Acceptor Polymers
(Collaboration with A. Abbotto – UniMIBI)

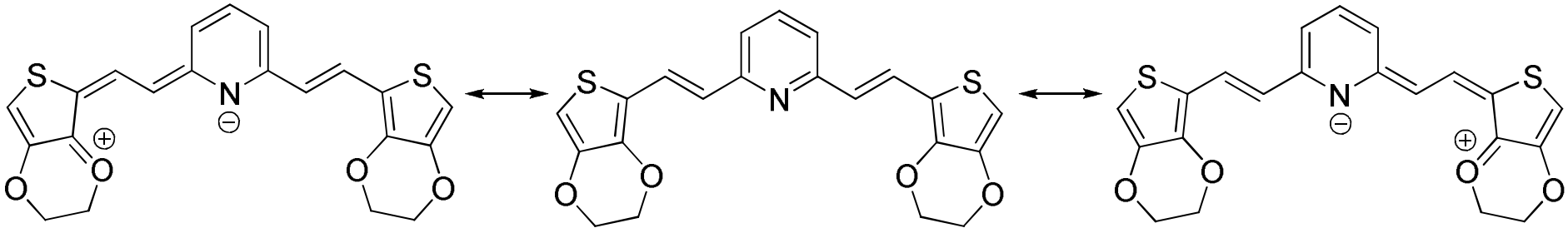

2,6-Py-V-EDOT

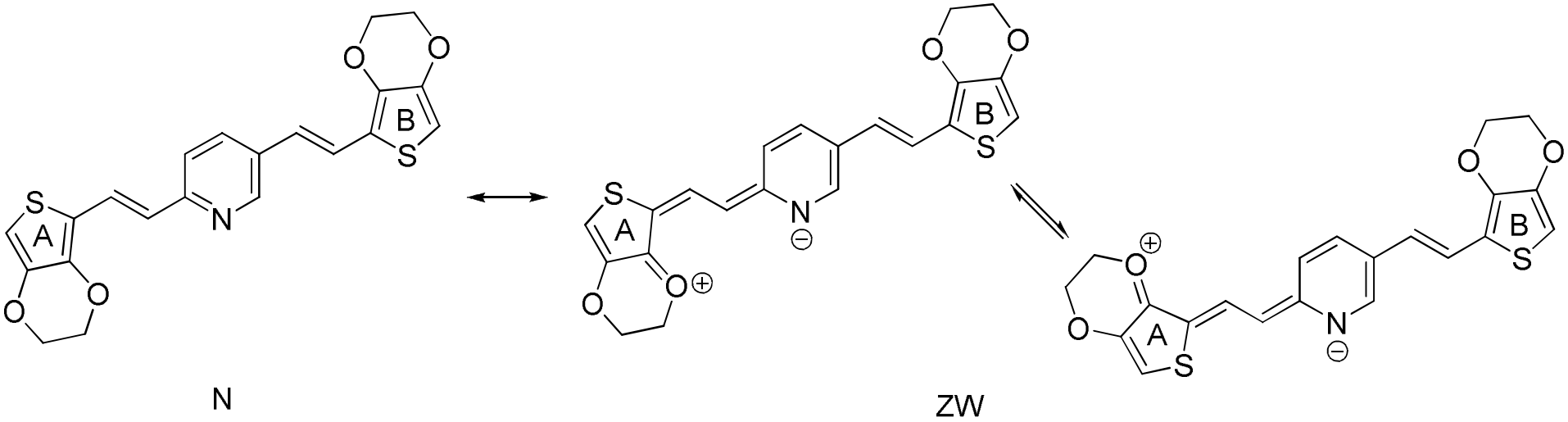

2,5-Py-V-EDOT

A. Abbotto, E. Herrera Calderon, M. S. Dangate, F. De Angelis, N. Manfredi, C. M. Mari, C. Marinzi, E. Mosconi, M. Muccini, R. Ruffo, M. Seri *Macromolecules*, **2010**, ASAP.

Computational investigation: From monomers to polymers

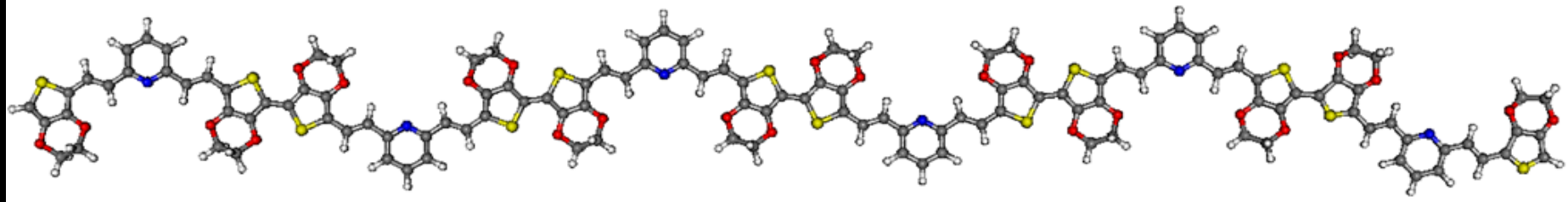

$P(2,6\text{-Py-V-EDOT})_{n=6}$

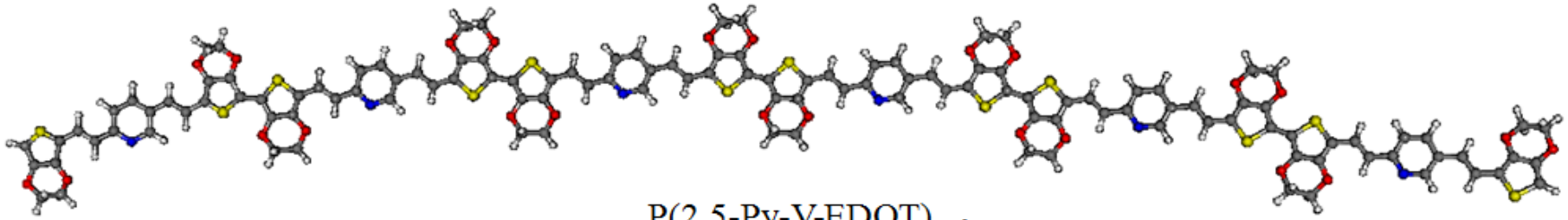

$P(2,5\text{-Py-V-EDOT})_{n=6}$

Evolution of the band-gap and of the HOMO and LUMO

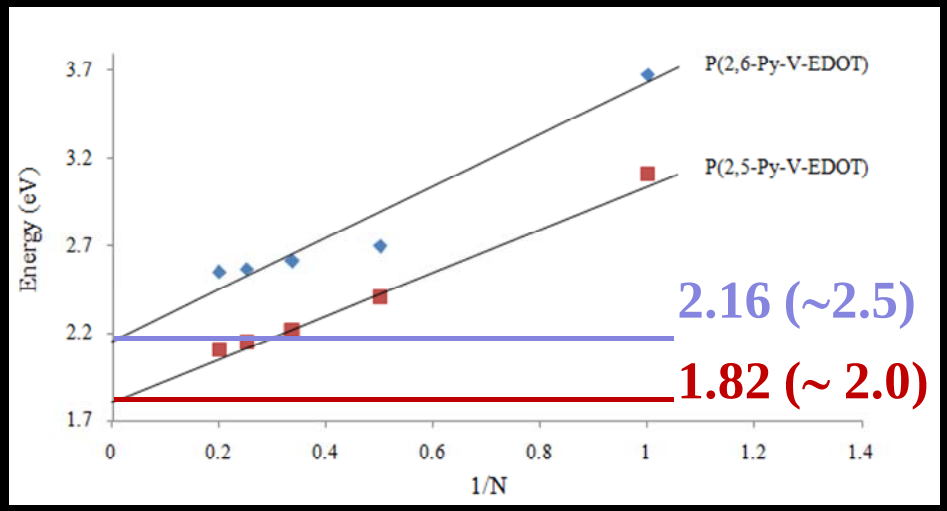

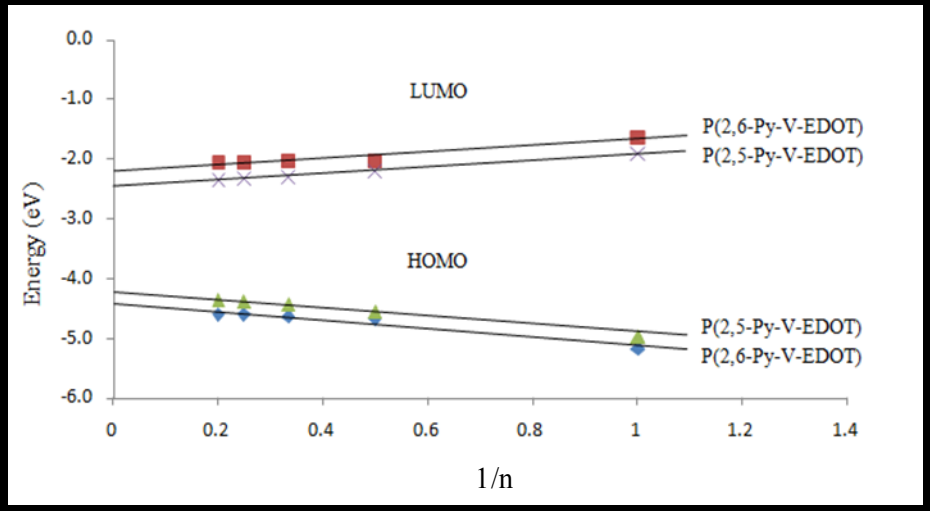

Computational investigation: Electronic structure of oligomers

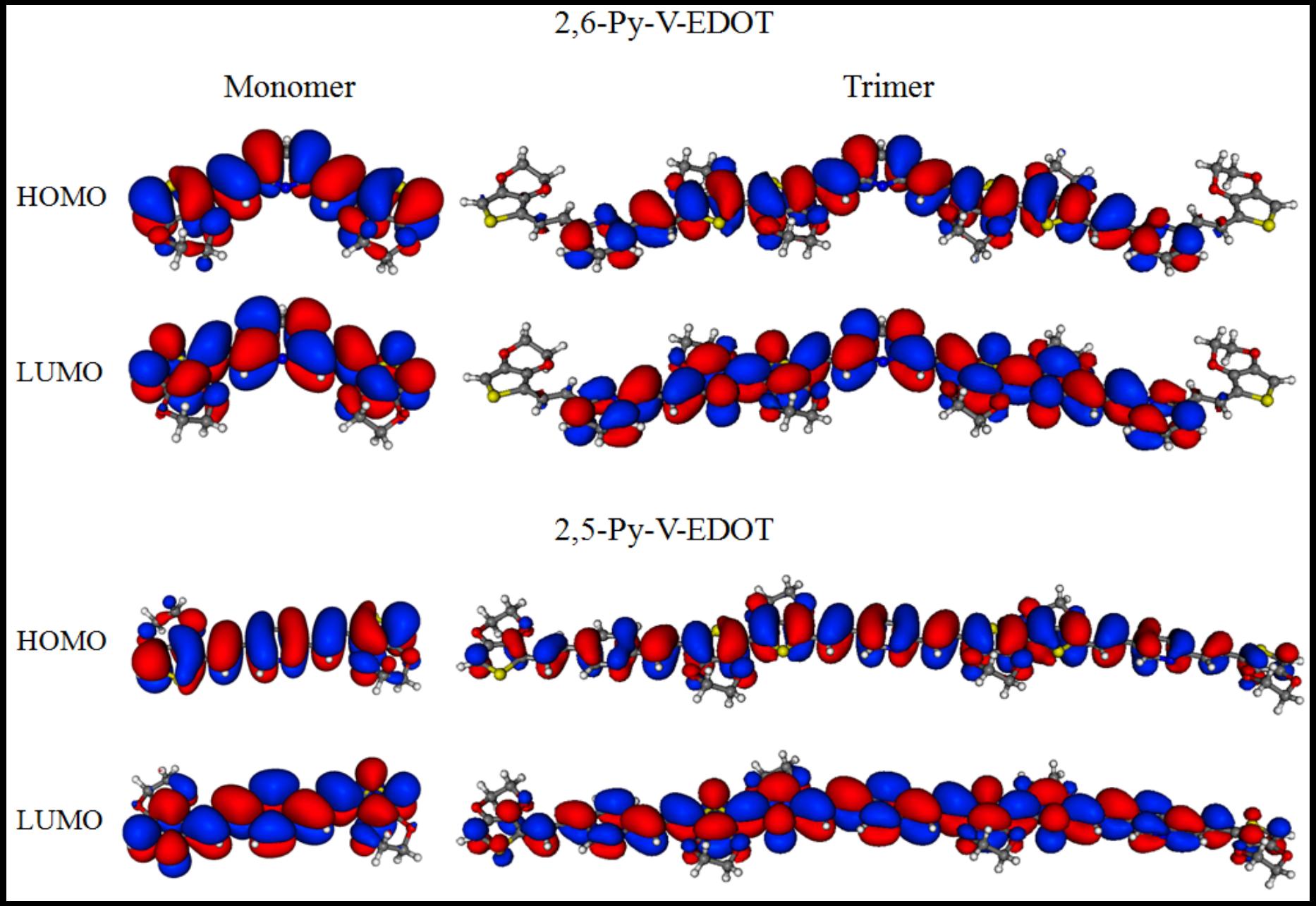

Anatase TiO_2 nanocrystals

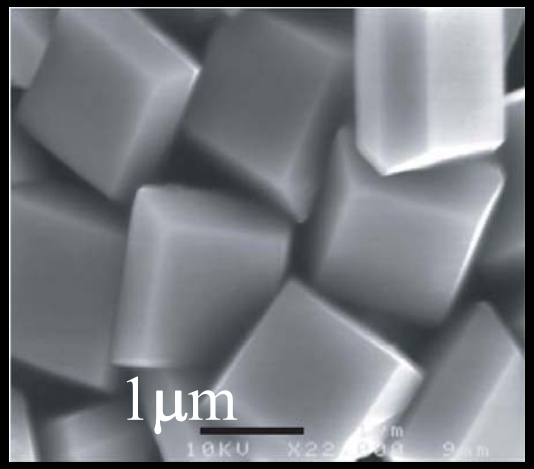

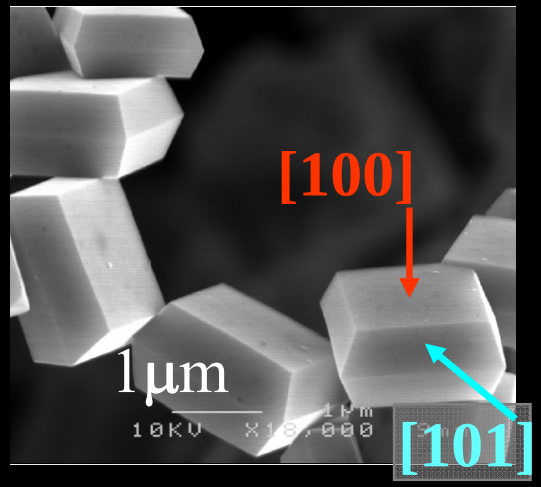

H. G. Yang et al. Nature 453, 2008, 29

Catal. Today 85, 2003,932

Truncated tetragonal bipyramidal shape:

two flat, square surfaces are [001] facets and eight isosceles trapezoidal surfaces are [101] facets.

The [101] is the most thermodynamically stable surface, while the [001] is more reactive for dissociative adsorption of reactant molecules.

High surface area and large reactive surface → higher photocatalytic activities.

Modeling of TiO_2 nanoparticles:

Stoichiometric anatase $(TiO_2)_{38}$ and $(TiO_2)_{82}$ clusters of 1 and 2 nm dimensions exposing (101) surfaces

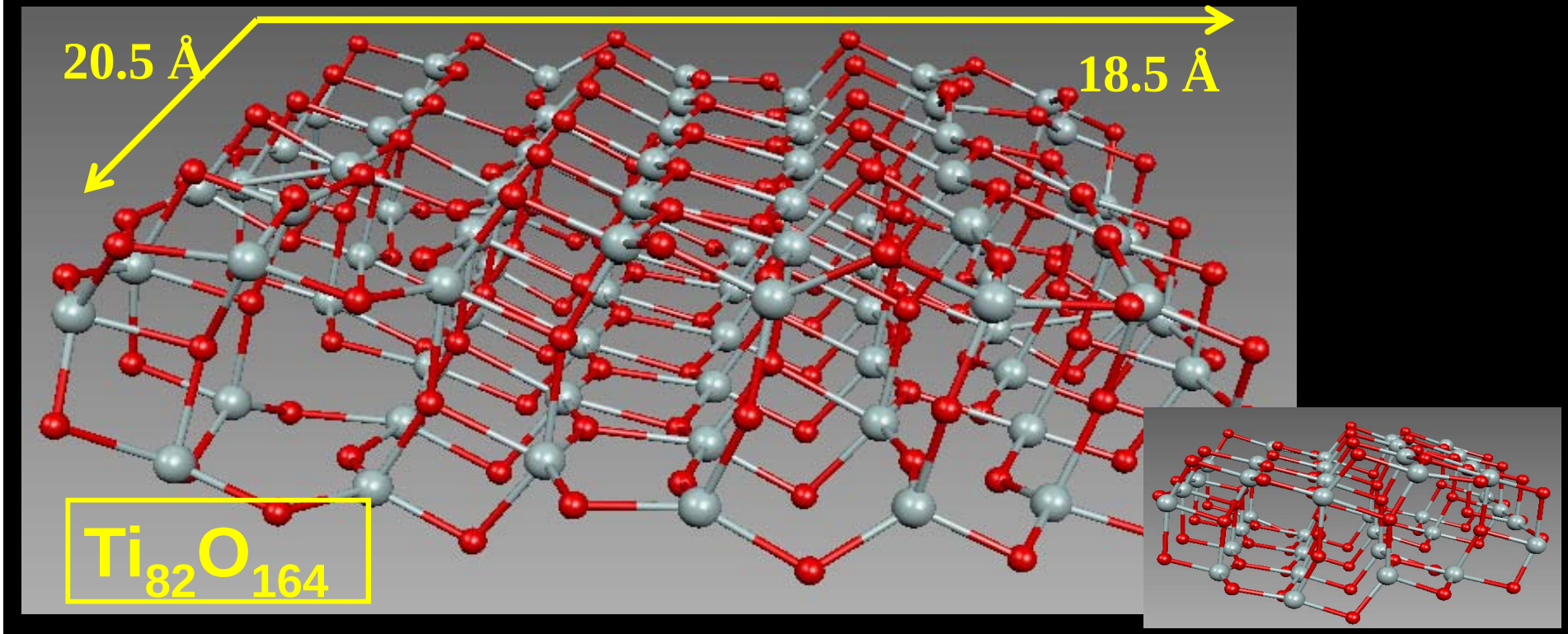

	B3LYP/3-21g*	B3LYP/DZVP
TD-DFT gap in water	3.20/3.41 eV	3.13/3.35 eV

Experimental gap in acqueous solutions: 3.20 – 3.30 eV

F. De Angelis, A. Tilocca, A. Selloni ***J. Am. Chem. Soc.*** **2004, *126*, 15024**

Realistic models of TiO_2 NTs and NCs

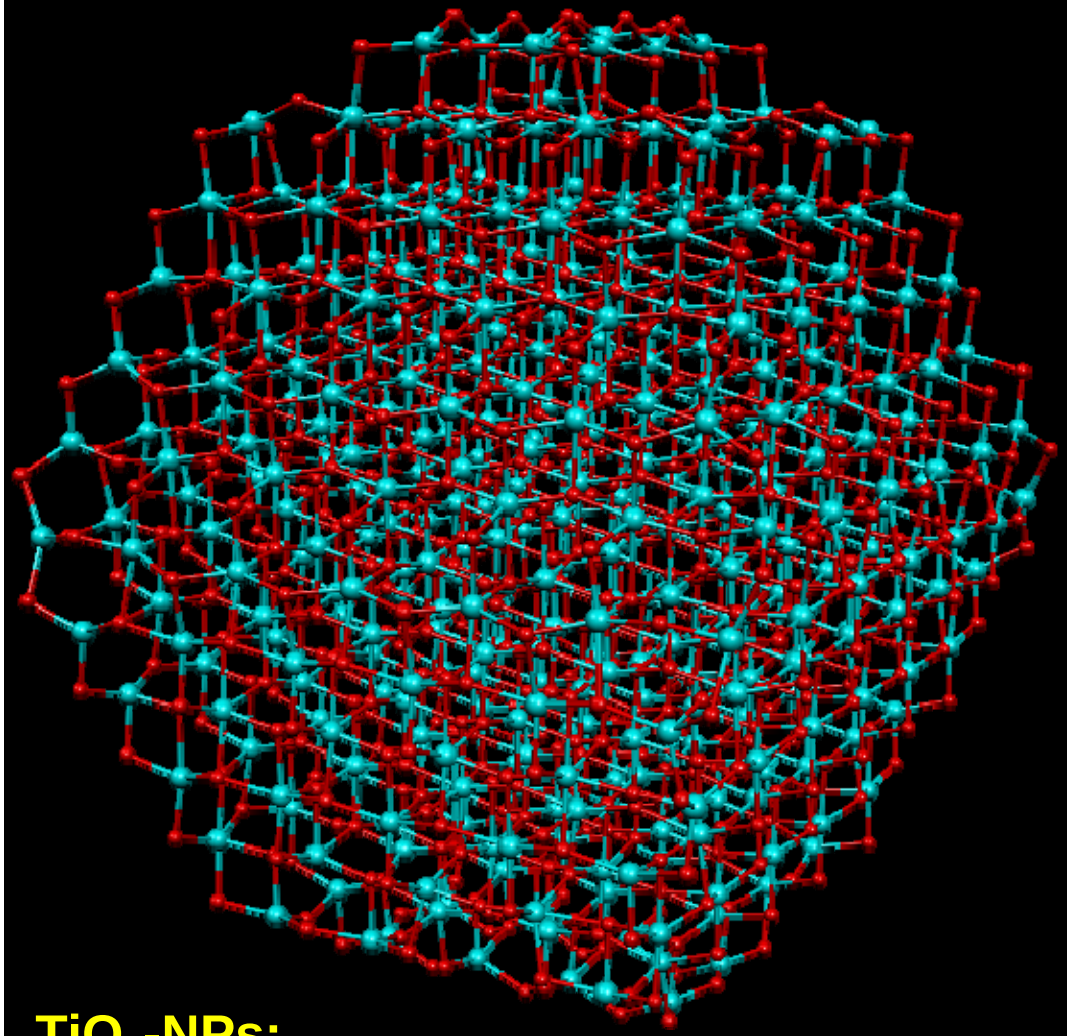

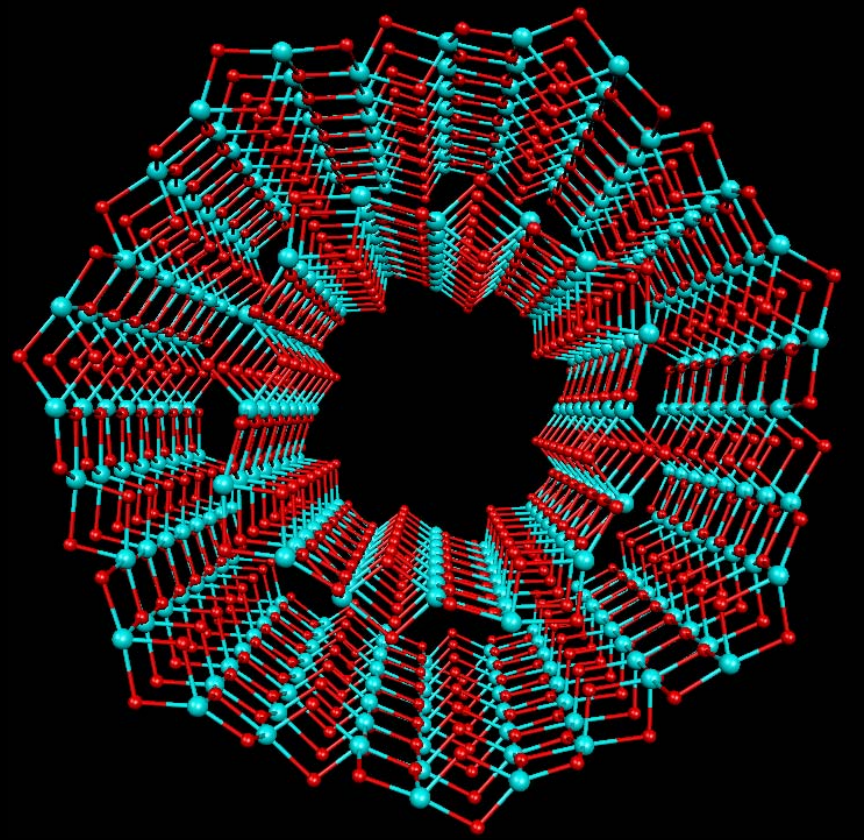

TiO_2-NPs:

Origin of sub-band gap states?

Single and Multi-Wall TiO_2-NTs:

Adsorption mode

Work in progress

F. Nunzi, F. De Angelis, ***J. Phys .Chem***. C, **2010**

Alignment of excited state potentials:

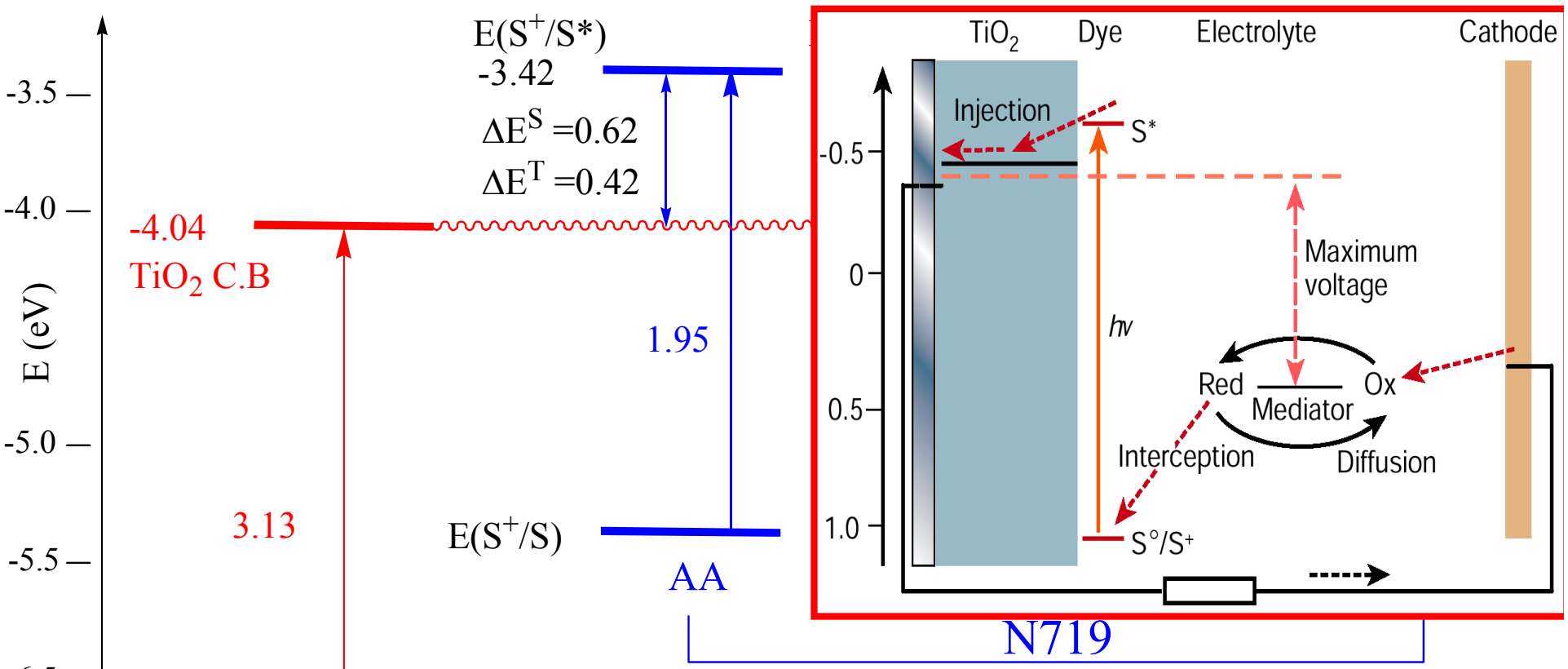

Exp.		Theor.
TiO_2 C.B	- 4.0/-4.2 eV	- 4.04 eV
TiO_2 vs. NHE	-0.50 V	
N719 vs. NHE	-0.98 V	(-3.42/-3.22 eV)
	ΔE =0.48 V	**ΔE^T =0. 435 eV**

F. De Angelis, S. Fantacci, A. Selloni, *Nanotechnology*, **2008**, *19*, 424002.

Ab initio molecular dynamics simulations

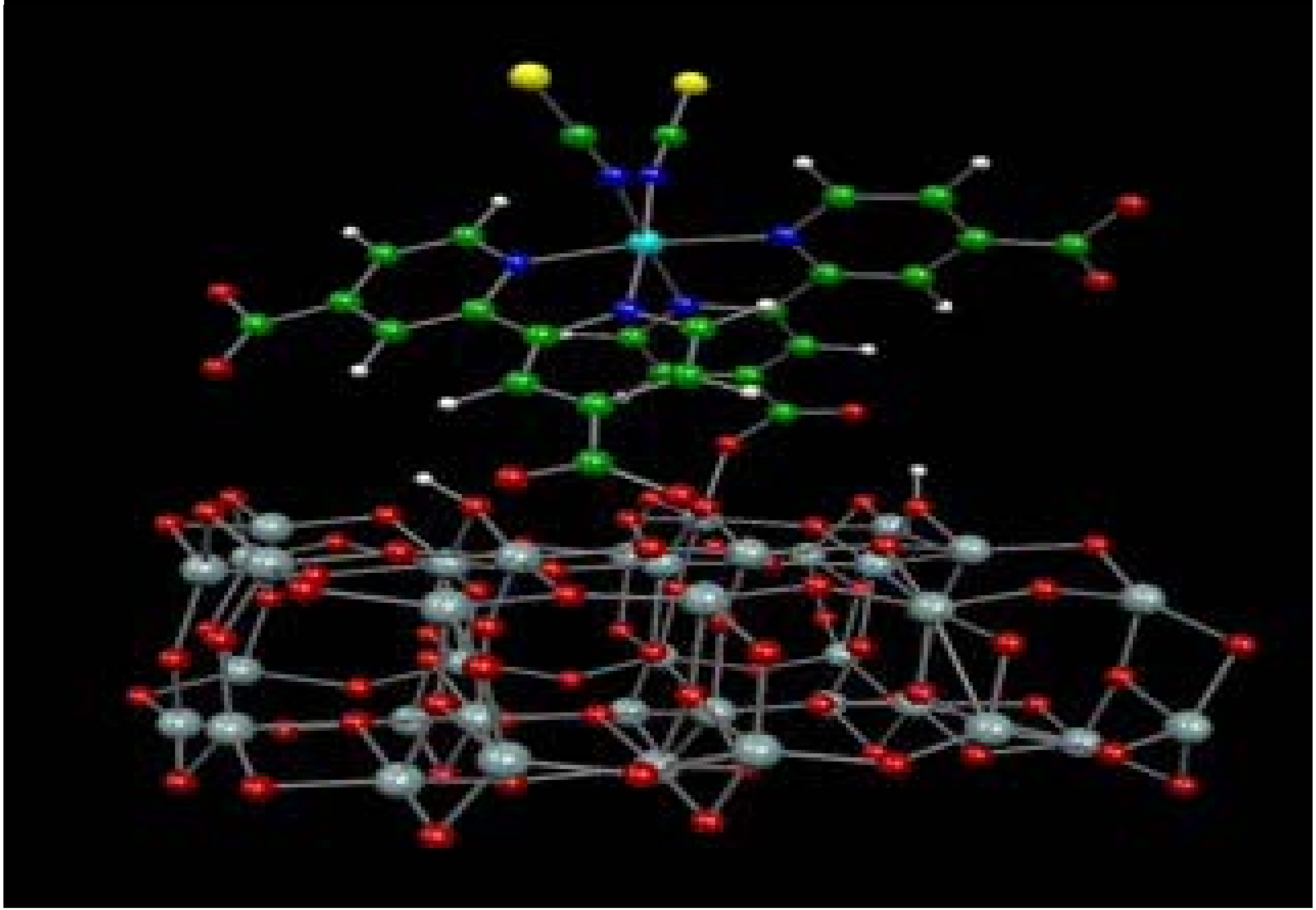

N719 adsorbed on TiO_2:

Two prototypical configurations of N719/TiO_2 were examined

The two protons are located on the dye (A) or on the TiO_2 (B)

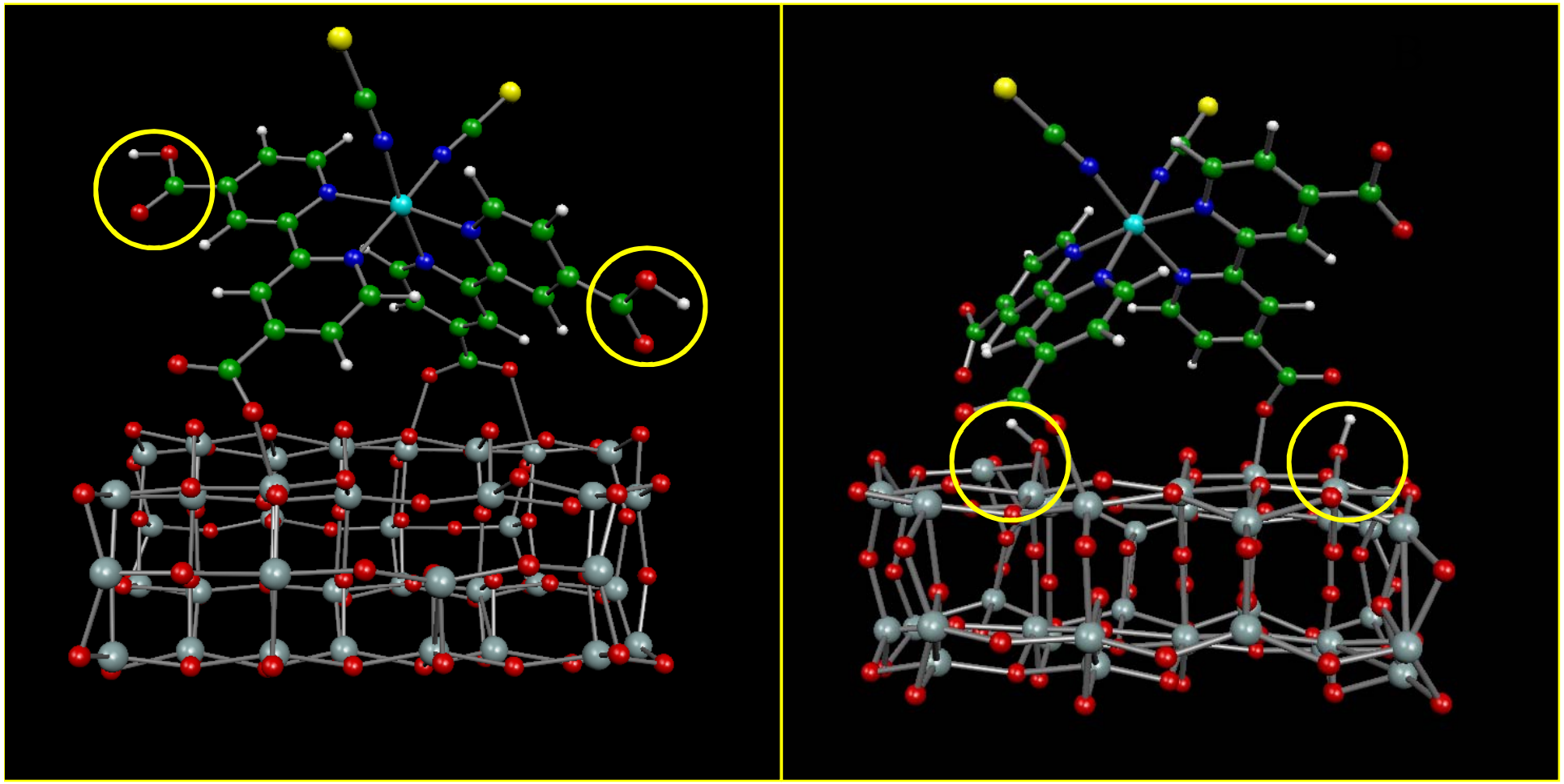

F. De Angelis, S. Fantacci, A. Selloni, M. Grätzel ***J. Am. Chem. Soc.*** *2007, 129, 14156.*

Electronic structure / number of H^+ on TiO_2

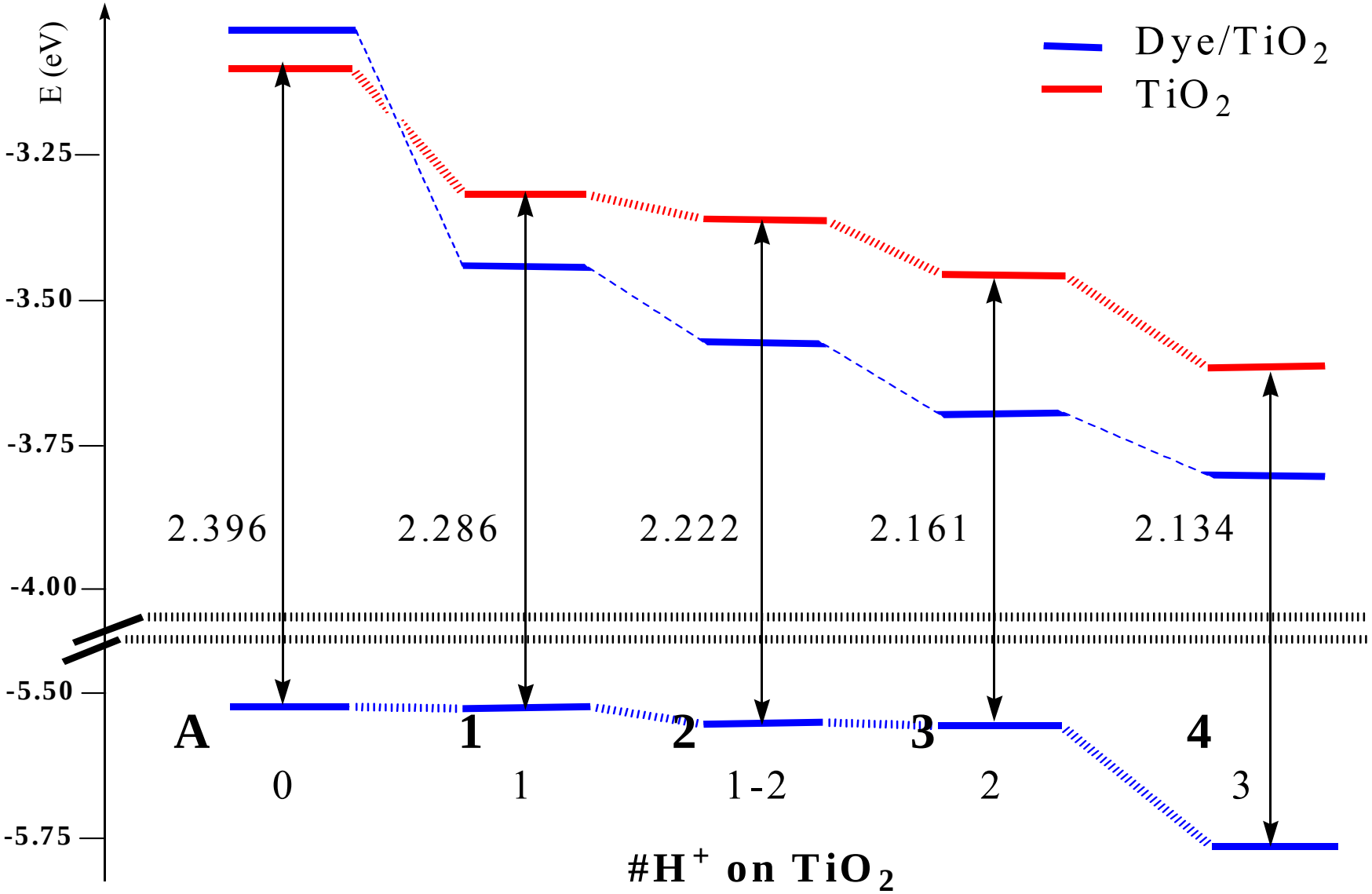

Increasing the protons on TiO_2 lowers the C.B. (and therefore V_{OC})

Md. K. Nazeeruddin, R. Humphry-Baker, P. Liska, M. Grätzel, *J. Phys. Chem. B,* **2003**, 107, 8981.

Charge generation and injection mechanisms:

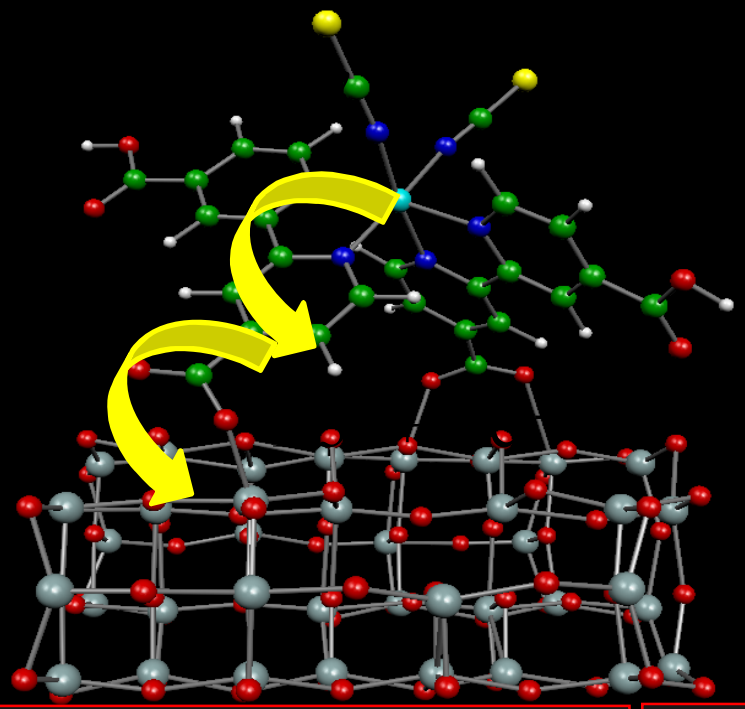

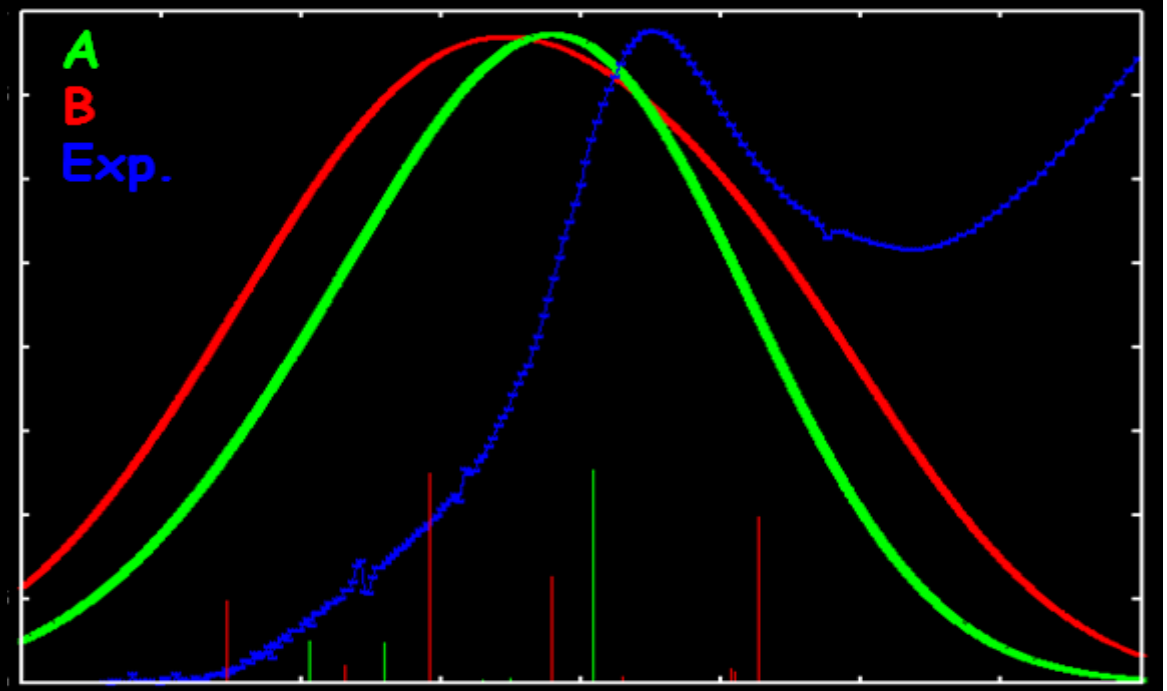

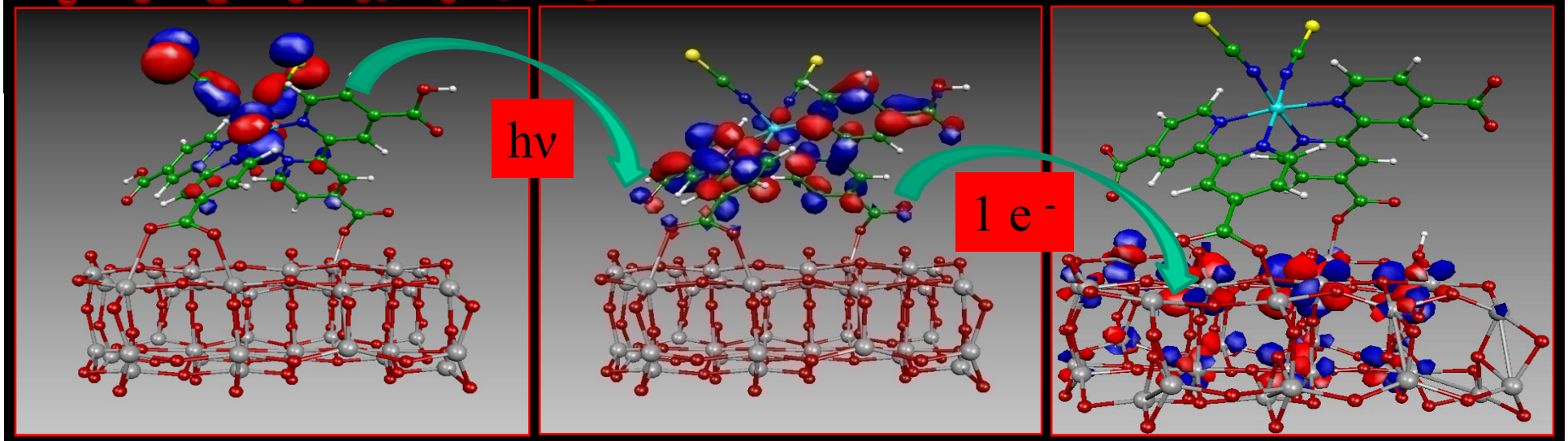

F. De Angelis, S. Fantacci, A. Selloni, M. Grätzel ***J. Am. Chem. Soc.*** *2007, 129, 10320.*

Tuning the properties of Ru(II) TiO_2 sensitizers

Control of protonation/ conuterions

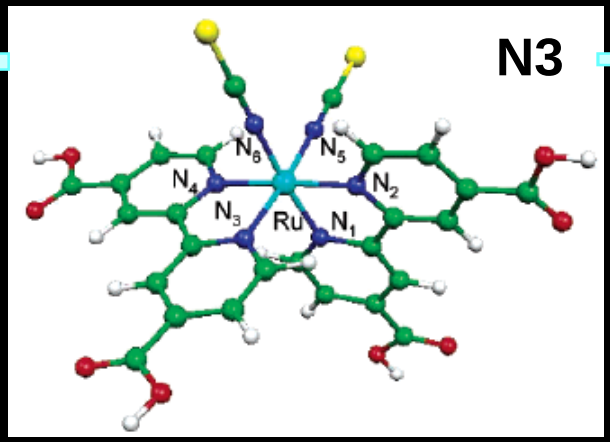

Stability/ Charge separation

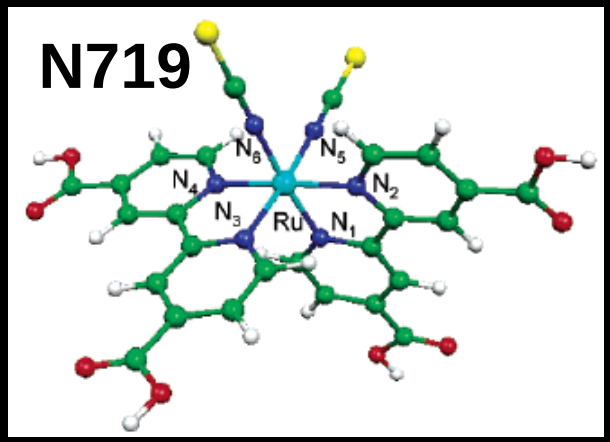

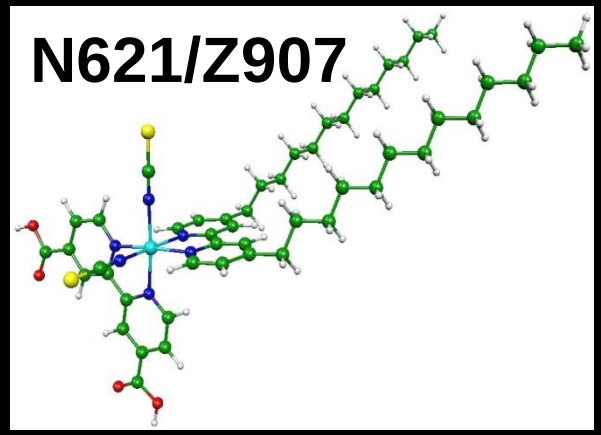

Ion-coordinating ligands

Improved light harvesting

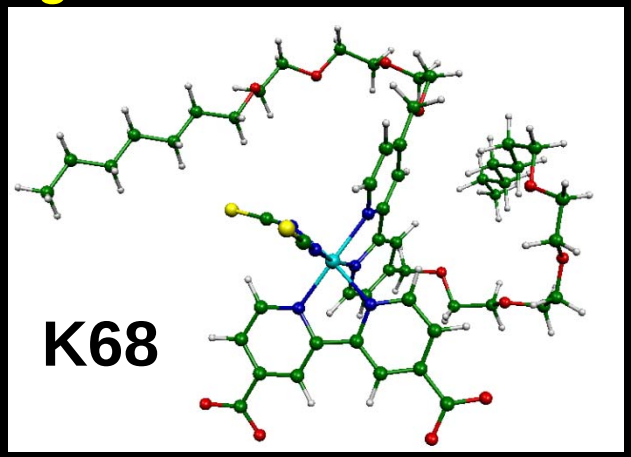

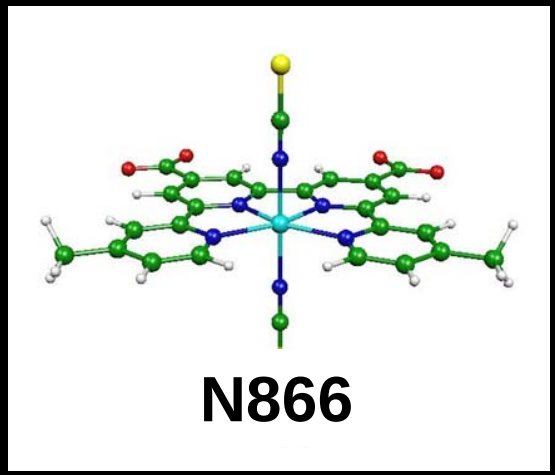

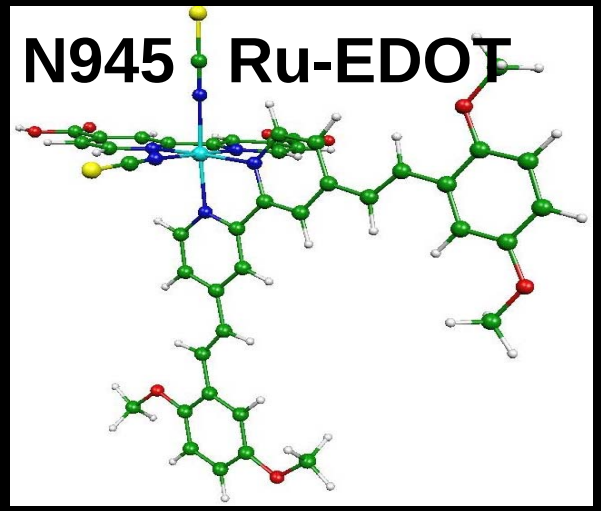

Quaterpyridil ligands
Trans isomers

Heteroleptic Ru(II) sensitizers: Ru-EDOT

High molar extinction coefficient ⇒ **High spectral response in the red**

Improved photovoltaic performances

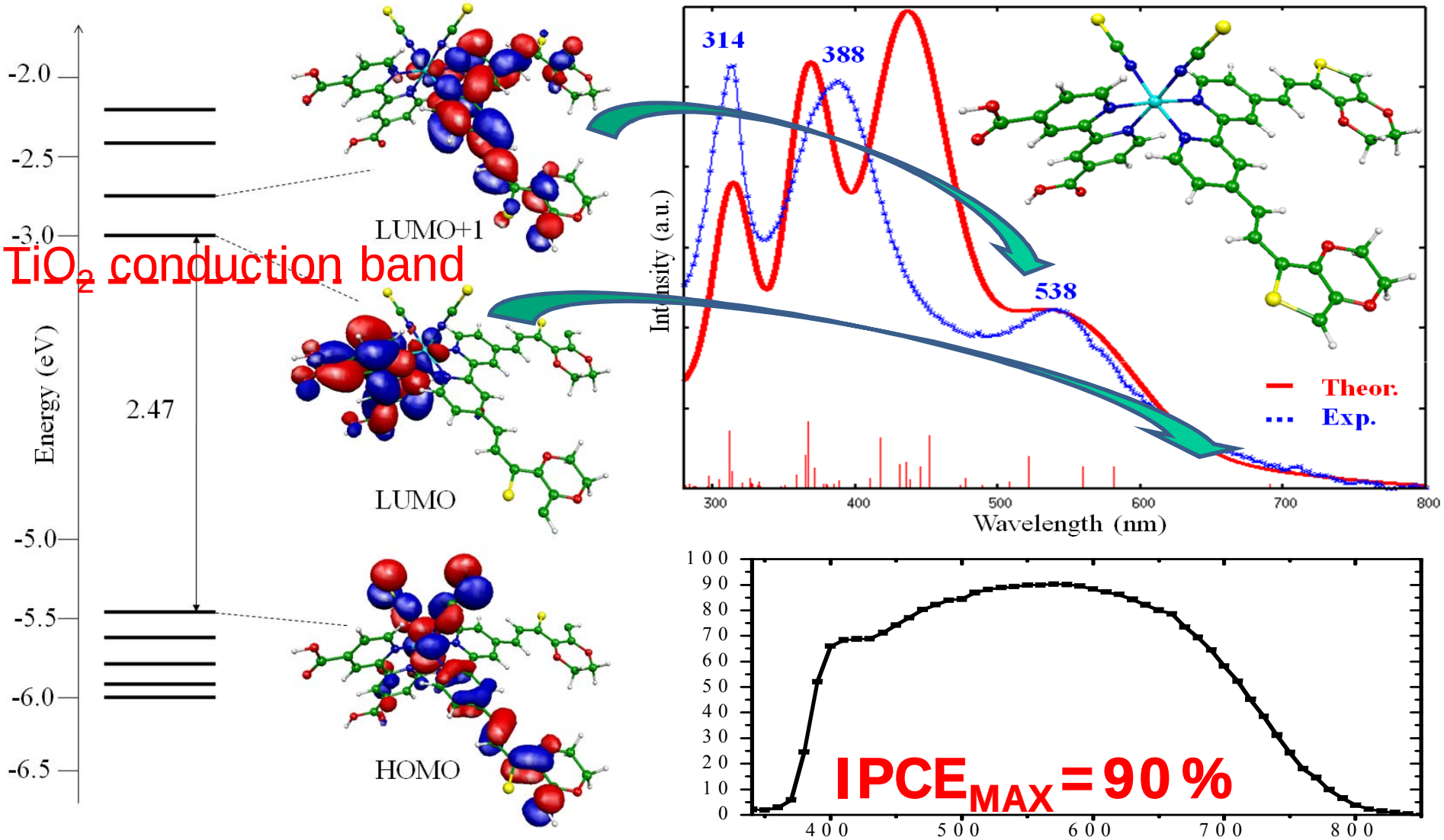

A. Abbotto, F. De Angelis, S Fantacci, M. Grätzel et al. *Chem Commun.* **2008,** 5318.

HOPV group Perugia

ICTP / SISSA Collaboration:

R. Gebauer, S. Baroni

Experiments at EPFL:

Md. K. Nazeeruddin, M. Grätzel

Financial support:

MIUR PRIN 2008 CNR EFOR 2011 IIT-SEED 2009

ESF HOPV 2010 EU-FP7: NMP-2009 ENERGY-2010